

## The lipoxygenase pathway of *Tupaia belangeri* representing *Scandentia*. Genomic multiplicity and functional characterization of the ALOX15 orthologs in the tree shrew



Marjann Schäfer<sup>a</sup>, Yu Fan<sup>b</sup>, Tianle Gu<sup>b,c</sup>, Dagmar Heydeck<sup>a</sup>, Sabine Stehling<sup>a</sup>, Igor Ivanov<sup>d</sup>, Yong-Gang Yao<sup>b,c</sup>, Hartmut Kuhn<sup>a,\*</sup>

<sup>a</sup> Institute of Biochemistry, Charité - University Medicine Berlin, Corporate member of Free University Berlin, Humboldt University Berlin and Berlin Institute of Health, Charitéplatz 1, D-10117 Berlin, Germany

<sup>b</sup> Key Laboratory of Animal Models and Human Disease Mechanisms of the Chinese Academy of Sciences & Yunnan Province, Kunming Institute of Zoology, Kunming, Yunnan 650223, China

<sup>c</sup> Kunming College of Life Science, University of Chinese Academy of Sciences, Kunming, Yunnan 650204, China

<sup>d</sup> Lomonosov Institute of Fine Chemical Technologies, MIREA - Russian Technological University, Vernadskogo pr. 86, 119571 Moscow, Russia

### ARTICLE INFO

#### Keywords:

Eicosanoids  
Tree shrew  
Evolution  
Phospholipids  
Biomembranes  
Oxidative stress  
Fatty acids

### ABSTRACT

The tree shrew (*Tupaia belangeri*) is a rat-sized mammal, which is more closely related to humans than mice and rats. However, the use of tree shrew to explore the patho-mechanisms of human inflammatory disorders has been limited since nothing is known about eicosanoid metabolism in this mammalian species. Eicosanoids are important lipid mediators exhibiting pro- and anti-inflammatory activities, which are biosynthesized *via* lipoxygenase and cyclooxygenase pathways. When we searched the tree shrew genome for the presence of cyclooxygenase and lipoxygenase isoforms we found copies of functional *COX1*, *COX2* and *LOX* genes. Interestingly, we identified four copies of *ALOX15* genes, which encode for four structurally distinct *ALOX15* orthologs (*tupALOX15a-d*). To explore the catalytic properties of these enzymes we expressed *tupALOX15a* and *tupALOX15c* as catalytically active proteins and characterized their enzymatic properties. As predicted by the Evolutionary Hypothesis of *ALOX15* specificity we found that the two enzymes converted arachidonic acid predominantly to 12S-HETE and they also exhibited membrane oxygenase activities. However, their reaction kinetic properties ( $K_M$  for arachidonic acid and oxygen, T- and pH-dependence) and their substrate specificities were remarkably different. In contrast to mice and humans, tree shrew *ALOX15* isoforms are highly expressed in the brain suggesting a role of these enzymes in cerebral function. The genomic multiplicity and the tissue expression patterns of tree shrew *ALOX15* isoforms need to be considered when the results of *in vivo* inflammation studies obtained in this animal are translated into the human situation.

### 1. Introduction

Lipoxygenases (ALOX-isoforms) are lipid peroxidizing enzymes [1–4], which are widely distributed in mammals [5] and higher plants [6]. Mammalian ALOX-isoforms have been implicated in cell differentiation and maturation but they also play a role in the pathogenesis of inflammatory, hyperproliferative, neurological and metabolic diseases [1–3]. During the inflammatory response ALOX-isoforms play a role for the biosynthesis of inflammatory mediators such as leukotrienes [7], lipoxins [8], resolvins [9] and hepxilins [10]. Knockout studies of different ALOX-isoforms in mice [11] suggested pro- and anti-inflammatory functions [12,13]. ALOX5 constitutes the key enzyme in the

biosynthesis of pro-inflammatory leukotrienes, which play a major role in anaphylactic reactions [14]. ALOX15 has been implicated in the biosynthesis of pro-resolving lipoxins [8], resolvins [9] and maresins [15] suggesting that *ALOX15* orthologs may play a role in inflammatory resolution. However, systemic knockout of the *Alox15* gene in mice induced pro- and anti-inflammatory effects depending on the inflammation model and these data suggest a dual role of these enzymes [16].

The Chinese tree shrew (*Tupaia belangeri chinensis*) is a small eutherian mammal that is native to Southeast Asia and Southwest China [17–19]. Phenotypically these animals resemble rats but evolutionarily they are more closely related to higher primates than the

\* Corresponding author at: Institute of Biochemistry (CC2), Charité - University Medicine Berlin, Charitéplatz 1, 10117 Berlin, Germany.

E-mail address: [hartmut.kuehn@charite.de](mailto:hartmut.kuehn@charite.de) (H. Kuhn).

frequently employed laboratory rodents [17–19]. They are characterized by a short life cycle, moderate size and easy feeding behaviours [18]. Their reproductive period begins 4 month after birth and typically, 2–6 offsprings are born each time [18]. From the evolutionary point of view, the tree shrews have been classified into the order of *Scandentia* [20], which consists of two families: *Tupaïidea* and *Ptilocercidea*. In 2012, the genome sequencing of the Chinese tree shrew was completed [21] and the sequence data showed that the nervous, immune and metabolic systems of the tree shrew were close to those of higher primates including humans [21]. Most recently, we worked out a high-quality chromosome-scale scaffolding of the Chinese tree shrew genome using long-read single-molecule sequencing and high-throughput chromosome conformation capture technology. These data corrected errors in earlier versions of the genome [22]. In addition, > 300 tree shrew proteins have been predicted to be drug targets for cancer chemotherapy, depression and cardio-vascular diseases [23]. In the past, the tree shrew has been used as an alternative to laboratory rodents to study the mechanisms of human diseases [18,24,25]. Unfortunately, the use of these animals to explore the mechanisms of human inflammatory disorders has currently been limited since for the time being little is known about the metabolism of eicosanoids and related lipid mediators in the Chinese tree shrews. In humans and other mammals eicosanoids are important lipid signalling molecules [26], which regulate the intensity of the inflammatory reaction. Some of them exhibit pro-inflammatory effects [7] but others initiate inflammatory resolution [9].

To fill this gap of knowledge and to test the suitability of the tree shrew to be employed as *in vivo* models for human inflammatory diseases, we searched the tree shrew genome for the presence of genes encoding for key enzymes of eicosanoid biosynthesis. We detected genes encoding for cyclooxygenase 1 (*COX1* = *PTGS1*), cyclooxygenase 2 (*COX2* = *PTGS2*) and different ALOX-isoforms. Interestingly, in contrast to most other mammals, which carry single copies of functional ALOX15 genes, the tree shrew genome involves four copies of the ALOX15 gene, which encode with high probability for functionally distinct enzyme isoforms. For this study, we expressed and functionally characterized two of the four tree shrew ALOX15 isoforms and compared their catalytic properties with those of mouse and human ALOX15. Although the biological roles of the tree shrew ALOX15 isoforms have not been explored in detail, the high expression levels in the brain suggest a cerebral function of these enzymes.

## 2. Results

### 2.1. Evolutionary position of the tree shrew

Mammals are classified in different superorders and one of them involves all superprimates (*Euarchontoglires*). *Euarchontoglires* are further subdivided into five orders (Fig. 1): *Rodentia*, *Lagomorphs* (together called *Glires*), *Scandentia*, *Primates*, *Dermoptera* (together called *Euarachonta*). Fig. 1 indicates that from the evolutionary point of view mice and rats, which are commonly employed as human disease models, are rather distant from humans. Thus, the Chinese tree shrew has been suggested as more suitable animal model for human disease models [18,19]. Unfortunately, our knowledge on the patho-mechanisms of inflammatory diseases in the Chinese tree shrews is rather limited, which prompted us to explore the lipoxygenase pathway in the tree shrew.

### 2.2. Identification of multiple copies of the ALOX15 gene in the tree shrew genome

In the genome of most mammals including humans, rats and mice a single copy of the ALOX15 gene is present. In contrast, when we searched the most updated version of the tree shrew genome [22] for the presence of ALOX15 genes we identified four different copies of the

ALOX15 gene (Table 1). All of them involve an open reading frame of 1992 nucleotides, which encode for 664 amino acids. When we compared the amino acid sequences of the four tree shrew ALOX15 isoforms (tupALOX15a, tupALOX15b, tupALOX15c, tupALOX15d) with the mouse ALOX15 ortholog (mouALOX15), we detected 67% of amino acid conservation (Table 2). The functionally important iron ligands were strictly conserved in all proteins (Fig. S1A) and the determinants for the reaction specificity were occupied by amino acids, which typically occur at these positions in 12-lipoxygenating ALOX15 orthologs [27]. Taken together, these data suggests with high probability that the corresponding enzymes are fully active 12-lipoxygenating ALOX15 isoforms. Interestingly, tupALOX15a and tupALOX15b shared a higher degree of amino acid conservation with humALOX15. When we compared the different tupALOX15 isoforms with each other (Table 2), we observed a very high degree of amino acid conservation. These data suggested a common origin of these genes. According to the amino acid similarity the four tupaia ALOX15 isoforms can be subgrouped in two separate families. On one hand tupALOX15a and tupALOX15b can be classified together whereas tupALOX15c and tupALOX15d form the second subfamily (Fig. S1B).

### 2.3. Expression of tupALOX15a and tupALOX15c in *E. coli*

To test the functionality of tupALOX15 isoforms we expressed tupALOX15a and tupALOX15c (representatives of the two tupALOX15 subfamilies) as recombinant N-terminal his-tag fusion proteins in *E. coli*. When we carried out SDS-PAGE (unspecific protein staining) with aliquots of the lysis supernatants we did not detect major differences between bacterial cultures transformed with recombinant and wildtype expression plasmids (data not shown). These data suggest that the two tupALOX isoforms are not highly expressed under our experimental conditions. However, when we carried out activity assays we observed the formation of specific ALOX products (Fig. 2A) and thus, the two recombinant tupALOX15 isoforms are successfully expressed in *E. coli*. For negative control experiments we employed the lysate supernatant of bacteria transformed with the “empty” plasmid (lacking the ALOX insert) for activity assays. Here we did not observe the formation of specific ALOX15 products. Similar results were obtained when the lysis supernatant of untransformed bacteria was used for activity assays.

The amounts of oxygenation products formed by tupALOX15a were almost 5-fold higher than that formed by tupALOX15c (Fig. 2A). These data suggest that tupALOX15a is either expressed at higher levels or that this isoenzyme exhibits a higher specific activity. To resolve this problem we carried out Western-blot analyses using an anti-his-tag antibody (Fig. 2B). When we applied identical volumes of the bacterial lysis supernatants to SDS-PAGE and stained the blots with an anti-his-tag antibody we found that tupALOX15a is expressed at 5-times higher levels (Fig. 2B). To estimate the expression levels of the two tree shrew ALOX isoforms (tupALOX15a and tupALOX15c) we calibrated the immunoblot intensity scale applying known amounts of purified his-tag *M. fulvus* ALOX [28] as calibration standard (see Materials and Methods for methodological details). Based on the relative band intensities we concluded that 12.7 mg tupALOX15a were expressed per liter liquid culture fluid. For unknown reasons the expression level of tupALOX15c was significantly lower (2.7 mg/L culture fluid). Taken together, these data indicate that the two tree shrew ALOX-isoforms are expressed at lower levels than the prokaryotic ALOX isoforms of *P. aeruginosa* [29] and *M. fulvus* [28] but at similar levels as other mammalian ALOX-isoforms [30,31].

The recombinant tree shrew ALOX15-isoforms migrated in SDS-PAGE with a molecular weight of 75,000 kDa (Fig. 2B), which is consistent with their theoretical molecular weight (75,205.55 Da for tupALOX15a and 75,155.51 Da for tupALOX15c) calculated from the protein sequences. To estimate the specific activities of the two enzymes equal volumes of lysis supernatant were employed for comparative activity assays. Here we found that the catalytic activity of

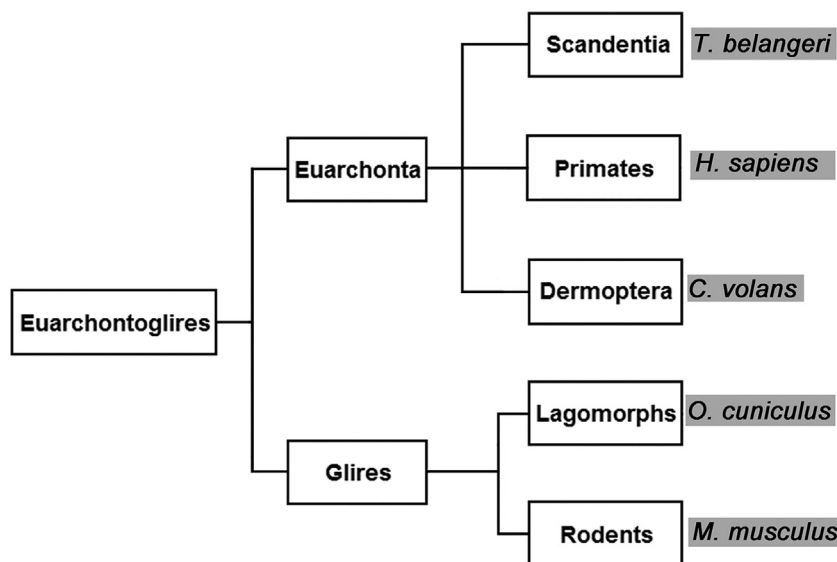


**Fig. 1.** Phylogenetic tree of Supraprimates (*Euarchontoglires*) visualizing the evolutionary relatedness of Primates (*humans*) and Scandentia (*tree shrew*). This presentation indicates that *H. sapiens* is more closely related to *T. belangeri* than to *M. musculus*.

**Table 1**

Exon/intron organization of the four different copies of tree shrew ALOX15 genes. The nucleotide sequences of the four ALOX15 genes present in the updated version of tree shrew genome were extracted from the tree shrew database ([www.treeshrewdb.org](http://www.treeshrewdb.org)) and the exon/intron organization was determined.

	Number of base pairs			
	ALOX15a	ALOX15b	ALOX15c	ALOX15d
Exon 1	135	138	135	135
Intron1	458	464	459	332
Exon 2	205	198	205	205
Intron 2	278	278	300	300
Exon 3	82	80	82	82
Intron 3	81	82	81	81
Exon 4	123	125	123	123
Intron 4	161	161	161	161
Exon 5	104	104	104	104
Intron 5	194	194	194	194
Exon 6	161	161	161	161
Intron 6	653	654	697	697
Exon 7	144	140	144	144
Intron 7	1.416	1.421	1.659	1.643
Exon 8	210	213	210	210
Intron 8	1.303	1.304	1.880	1.899
Exon 9	87	87	87	87
Intron 9	93	93	93	93
Exon 10	170	171	170	170
Intron 10	155	152	155	155
Exon 11	122	124	122	122
Intron 11	555	856	553	555
Exon 12	101	101	101	101
Intron 12	110	111	110	110
Exon13	168	169	168	168
Intron 13	103	104	103	103
Exon 14	180	181	180	180
Intron 14	996	997	997	997
Sum in exons	1.992	1.992	1992	1.992

tupALOX15a was about 4-fold higher than that of tupALOX15c (Fig. 2A) and immunoblotting indicated a five-fold higher expression of tupALOX15a. Combining these data, we concluded that the two tupALOX15 isoforms exhibit a similar specific arachidonic acid activity.

Finally, we attempted to purify the two enzymes from the bacterial lysates supernatant by affinity chromatography on Ni-agarose. Both enzymes bind to the Ni-agarose matrix but we were unable to recover

catalytically active protein of tupALOX15c when washing the affinity columns with increasing imidazole concentrations. Thus, we decided to characterize the catalytic properties of the two enzymes using the bacterial lysis supernatants as enzyme source.

#### 2.4. Functional characterization of recombinant tree shrew ALOX15 orthologs

Mammalian ALOX15 orthologs exhibit dual reaction specificity and 12- and 15-HETE have previously been identified as major arachidonic acid oxygenation products [31–33]. To explore the reaction specificities of the two tree shrew ALOX15 isoforms we analyzed the product pattern formed during a 3 min incubation period. RP-HPLC analysis (Fig. 3) of the oxygenation products indicated that both enzymes oxygenate arachidonic acid to conjugated dienes, which co-chromatograph in RP-HPLC with authentic standards of 12- and 8-HETE. Unfortunately, these two products are not well resolved under our experimental conditions. As minor oxygenation, which accounts for about 10% of the sum of the oxygenation products, conjugated dienes co-migrating with an authentic standard of 15-HETE were also detected. To obtain more detailed information on the chemical structure of the reaction products, the conjugated dienes formed were prepared by RP-HPLC and further analyzed by NP-HPLC and CP-HPLC. Here we found that neither of the two enzymes formed significant amounts of 8-HETE (left insets to Fig. 3). Thus, the major arachidonic acid oxygenation product was 12-HETE. Chiral phase HPLC (right insets to Fig. 3) indicated a strong preponderance of 12S-HETE over the corresponding 12R-enantiomer indicating that the stereochemistry of 12-HETE formation was completely enzyme controlled. For 15-HETE formed by tupALOX15c we also analyzed the enantiomer composition (lower right inset, Fig. 3) and we found a lower degree of stereocontrol (15SHETE/15R-HETE ratio of about 2:1). These data indicate that the two tree shrew ALOX15 isoforms are arachidonic acid 12S-lipoxygenating enzymes and thus, they follow the evolutionary concept of the reaction specificity of mammalian ALOX15 orthologs [5,27].

To quantify the substrate affinity of the two tree shrew ALOX15 isoforms for arachidonic acid their catalytic activities were measured at different substrate concentrations. From Fig. 4 it can be seen that the two enzymes follow Michaelis-Menten kinetics and  $K_M$ -values of 232  $\mu\text{M}$  and 116  $\mu\text{M}$  were determined for tupALOX15a and tupALOX15c, respectively. For native rabbit ALOX [34] and for recombinant ALOX from *Pseudomonas aeruginosa* [35] much higher substrate

**Table 2**

Degree of amino acid conservation of tree shrew ALOX15 isoforms (tupALOX15) compared with mouse ALOX15 (mouALOX15). The protein sequence of mouALOX15 was retrieved from the NCBI protein database and sequences of the tupALOX15 isoforms were retrieved from the updated version of the tree shrew genome ([www.treeshrewdb.org](http://www.treeshrewdb.org)). The degrees of amino acid identity were calculated using an online tool ([https://www.ebi.ac.uk/Tools/psa/emboss\\_needle/](https://www.ebi.ac.uk/Tools/psa/emboss_needle/)).

	Degree of amino acid identity (%)				
	mouALOX15	tupALOX15a	tupALOX15b	tupALOX15c	tupALOX15d
mouALOX15	100	67.1	66.6	66.8	67.1
tupALOX15a	67.1	100	97.6	98.0	96.5
tupALOX15b	66.6	97.6	100	95.6	94.7
tupALOX15c	66.8	98.0	95.6	100	97.0
tupALOX15d	67.1	96.5	94.7	97.0	100

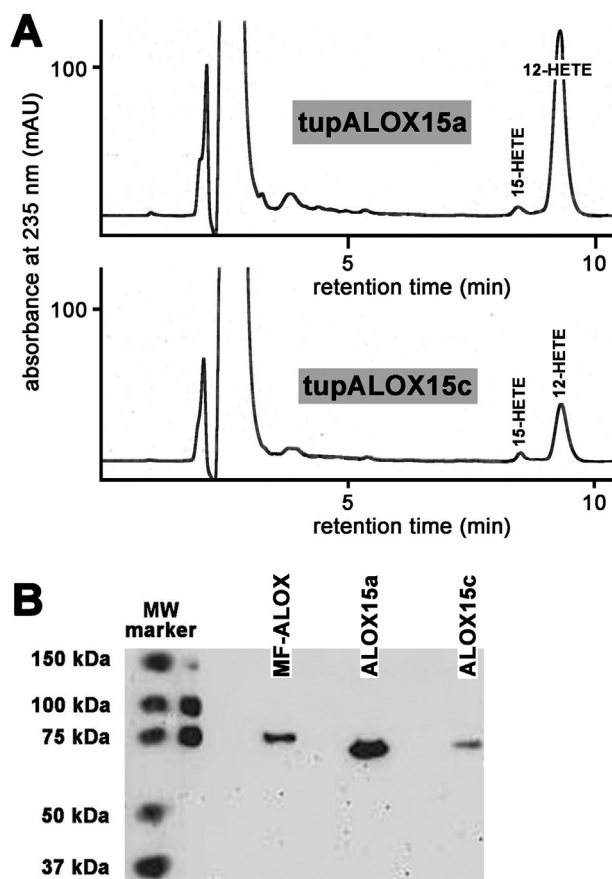


**Fig. 2.** Expression of tupALOX15a and tupALOX15c in *E. coli*. Tree shrew ALOX15 isoforms tupALOX15a and tupALOX15c were expressed in *E. coli* as described in the Mat + Meth section and the bacterial lysis supernatant was used as enzyme source. Activity assays were carried out as described in the Mat + Meth section and 20  $\mu$ L of lysis supernatant were employed as enzyme source. A) Arachidonic acid activity assay using 20  $\mu$ L tupALOX15a (upper trace) and 20  $\mu$ L tupALOX15c (lower trace) as enzyme. Retention times of authentic standards are given above the chromatographic traces. Activity assays were carried out in triplicate and a representative RP-HPLC chromatogram is shown. B) Immunoblot analysis of bacterial lysis supernatants for recombinant expression of tupALOX15 isoforms. 6  $\mu$ L of lysis supernatants were applied to SDS-PAGE and the blots were developed as indicated in the Mat + Meth section. For standardization purpose known amounts (250 and 500 ng) of purified *M. fulvus* ALOX (MF-LOX) was also taken through the analytical protocol.

affinities have previously been published. However, these measurements were carried out in the presence of detergents, which improves the water solubility of the substrates [29] and thus, lowers the  $K_M$ .

Lipoxygenase catalysis is a bimolecular reaction that requires oxygen as second substrate. Most ALOX isoforms exhibit a high oxygen affinity with  $K_M$ -values for oxygen in the lower  $\mu$ M range [36].

However, for recombinant ALOX of *Pseudomonas aeruginosa* an oxygen  $K_M$  of  $> 400 \mu$ M was determined [37], which is far above the physiological range of oxygen concentrations in biological fluids. ALOX-isoforms with such low oxygen affinities might function as oxygen sensing proteins. To compare the oxygen affinities of the two tree shrew ALOX15 isoforms we carried out activity assays at different oxygen concentrations and quantified the product formation by RP-HPLC. Care was taken that even under the lowest oxygen concentrations the amounts of reaction products formed were rather low so that the reaction sample did not turn anaerobic during the incubation period. From Fig. 5 it can be seen that the two enzymes follow Michaelis-Menten kinetics and that the oxygen  $K_M$  for tupALOX15a was 18.5  $\mu$ M. This value is in the range of oxygen  $K_M$  values of other mammalian ALOX-isoforms [34,36,38]. On the other hand, tupALOX15c exhibits a lower oxygen affinity (87.4  $\mu$ M). Thus, under physiological oxygen concentrations, this enzyme does not react at  $V_{max}$  conditions and alterations in the intracellular oxygen concentrations will affect the catalytic efficiency of the enzyme. It is possible, that this ALOX15 isoform functions as oxygen sensor as it has been suggested for the ALOX isoform of *Pseudomonas aeruginosa* [37].

Next, we studied the pH-dependence of the two tree shrew ALOX15 isoforms (Fig. 6). For both enzymes, rather flat bell-shaped curves were observed with  $pH_{opt}$  values in the physiological range. Interestingly, for tupALOX15a the bell-shaped curve is somewhat dislocated to more acidic pH-values whereas the curve for tupALOX15c appears to be shifted to the alkaline range.

The temperature profiles for the two tree shrew ALOX15 isoforms are shown in Fig. 7. tupALOX15a showed an optimal reaction temperature at 15  $^{\circ}$ C and at higher temperatures, the reaction rate declined. In contrast, we observed an increase in the reaction rate for tupALOX15c until 25  $^{\circ}$ C. These data suggest that tupALOX15a is apparently more sensitive to temperature-induced denaturation. In contrast, tupALOX15c is apparently more heat stable. When we constructed an Arrhenius plot from the activity data in the temperature range between 5 and 15  $^{\circ}$ C for tupALOX15, we calculated an activation energy of 14.9 kJ/mol. This value is somewhat lower than that determined for soybean LOX1 [39], rabbit ALOX15 [40] and the quasi-LOX activity of hemoglobin [41]. For the ALOX isoforms of *P. aeruginosa* [29] and *M. fulvus* [28] higher activation energies have been determined. For tupALOX15c, we constructed the Arrhenius plot in the temperature range 5  $^{\circ}$ -25  $^{\circ}$ C and obtained an activation energy of 82.5 kJ/mol. This value is in the range of the activation energies determined for the two prokaryotic ALOX isoforms [28,29].

Most ALOX isoforms identified so far exhibit a broad substrate specificity accepting several polyenoic fatty acids as substrate. To compare the substrate specificity of tupALOX15a and tupALOX15c we incubated the two enzymes with the most abundant mammalian polyenoic fatty acids [linoleic acid (LA), alpha-linolenic acid (ALA), gamma-linolenic acid (GLA), arachidonic acid (AA), eicosapentaenoic acid (EPA) and docosahexaenoic acid (DHA)] for 3 min and quantified the amounts of conjugated dienes formed during the incubation period by HPLC. From Fig. 8 it can be seen that LA is the best substrate for

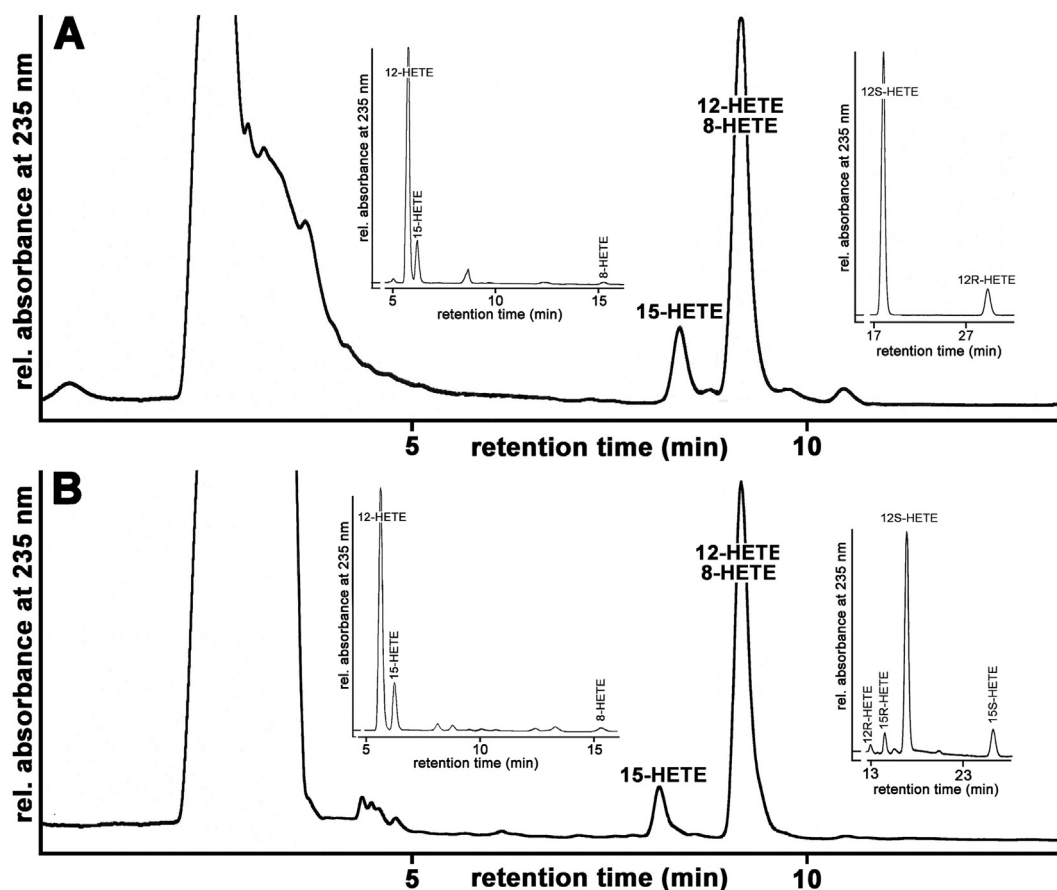


**Fig. 3.** Identification of the chemical structure of the arachidonic acid oxygenation products formed by tupALO15a and tupALO15c. Tree shrew ALOX15 isoforms (tupALO15a and tupALO15c) were expressed in *E. coli* and activity assays were carried out as described in the Mat + Meth section. The reaction products were analyzed by RP-HPLC recording the absorbance of the column effluent at 235 nm. The conjugated dienes eluted in the hydroxy fatty acid region (7–10 min) were prepared and further analyzed by NP-HPLC (left insets). Here again, the major conjugated dienes were prepared and further analyzed by CP-HPLC (right inset, upper trace) or by combined NP/CP-HPLC (right inset, lower trace). Activity assays were carried out in triplicate for each enzyme and a representative RP-HPLC chromatogram is given. For NP- and CP-HPLC (insets), the conjugated dienes of all activity assays were pooled and analyzed together.

tupALO15a followed by GLA, AA and EPA. ALA and DHA are less well oxygenated. In contrast, GLA is the best substrate for tupALO15c followed by LA and AA. ALA, EPA and DHA are not well oxygenated.

As indicated in Fig. 3 AA is oxygenated by tree shrew ALOX15a and tupALO15c with dual positional specificity to 12-H(p)ETE (n-9 oxygenation) and 15-H(p)ETE (n-6 oxygenation) in a ratio of about 9:1. These data suggest the principle capability of the two enzymes to catalyze hydrogen abstraction from the bisallylic carbon atoms C10 [n-9 hydrogen abstraction for 12-H(p)ETE formation] and C13 [n-6 hydrogen abstraction for 15-H(p)ETE formation]. To explore, which products are formed from other polyenoic fatty acids, the major conjugated dienes formed from different substrates were analyzed by RP-HPLC and GC-MS. As expected from the similar patterns of arachidonic acid oxygenation products (Fig. 3) generated by tupALO15a and tupALO15c we did not find major differences in the product patterns of the two enzymes using the other polyenoic fatty acids as substrate. In fact, the RP-HPLC chromatograms shown in Fig. 9 for tupALO15a looked almost identical for tupALO15c. To explore the structure of the major oxygenation products, the conjugated dienes were prepared by RP-HPLC and further analyzed by GC-MS. As indicated in Fig. 9A linoleic acid (LA) is converted to a single conjugated diene and the major fragmentation ions observed in GC-MS (Table 3) indicate the chemical identity of this compound as 13-HODE (n-6 oxygenation). ALA is also oxygenated to a single conjugated diene (Fig. 9B) and the alpha-cleave ions indicate 13-HOTrE(n-3) as dominant reaction product (n-6 oxygenation). LA and ALA do not carry n-11 bisallylic methylenes and thus, the formation of n-9 oxygenation products is impossible. In

contrast, the substrates, which carry both n-8 and n-11 bisallylic methylenes, are oxygenated with dual reaction specificity. For instance, GLA (Fig. 9C), which involves both n-8 (C11) and n-11 (C8) bisallylic methylenes, was oxygenated to an 8:2 mixture of 10-H(p)OTrE(n-6) (late eluting conjugated diene (b) in Fig. 9C) and 13-H(p)OTrE(n-6) (early eluting minor conjugated diene (a) in Fig. 9C). A similar situation was observed for DHA (Fig. 9E). Here the early eluting minor conjugated diene (a) was identified as 17-HDHA (n-6 oxygenation, hydrogen abstraction from the n-8 bisallylic methylene C15). In contrast, the late eluting diene (b) was identified as 14-HDHA (n-9 oxygenation, hydrogen abstraction from the n-11 bisallylic methylene C12). For EPA (Fig. 9D) we observed a pronounced dual specificity for the two tree shrew ALOX15 isoforms. The early conjugated diene (a) was identified as 15-HEPE and the late eluting product (b) as 12-HEPE (Table 3).

### 2.5. Membrane oxygenase activity of tree shrew ALOX15 isoforms

ALOX15 orthologs of different species are capable of oxygenating polyenoic fatty acids even if they are esterified in membrane phospholipids or lipoprotein cholesterol esters [3,42–44]. To test whether tree shrew ALOX15 isoforms also exhibit a membrane oxygenase activity we incubated *in vitro* different amounts of enzymes with mitochondrial membranes and analyzed by HPLC the oxygenation products in the hydrolyzed lipid extracts. Following the chromatograms of a non-enzyme control incubation at 235 nm (Fig. 10A, upper trace), we observed the presence of an unknown compound, which eluted with a retention time of about 8 min. Its UV-spectrum (inset I to Fig. 10A) with

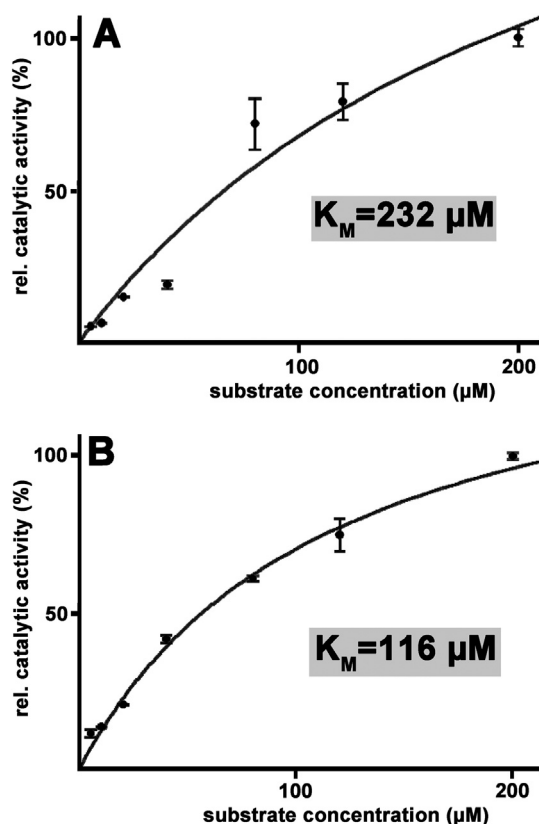


**Fig. 4.** Reaction kinetics of arachidonic acid oxygenation by tree shrew ALOX15 isoforms. Tree shrew ALOX15 isoforms (tupALOX15a and tupALOX15c) were expressed in *E. coli* and activity assays were carried out at different substrate concentrations as described in the Mat + Meth section. The mean of the reaction rate measured at the highest substrate concentration was set 100%. A) tupALOX15a, B) tupALOX15c. Activity assays at each substrate concentration were carried out in duplicate and means and standard errors are given.

its two local absorbance maxima at 215 and 273 nm indicated that this compound does not represent a primary fatty oxygenation product. Based on the chromatogram at 210 nm (lower trace in Fig. 10A) we analyzed the non-oxygenated polyenoic fatty acids (PUFAs). As expected AA (early eluting peak) and LA (late eluting peak) were identified as major polyenoic fatty acids of mitochondrial membranes [43]. When we analyzed at 235 nm the hydrolyzed lipid extracts of the samples, in which the membranes had been incubated with tupALOX15a, we observed two additional peaks, which eluted in the region of hydroxy fatty acids. These two additional peaks (Fig. 10B), which coeluted with authentic standards of 13-HODE (early eluting compound) and 12-HETE (late eluting compound), carried a conjugated diene chromophore (inset II to Fig. 10A). To analyze the chemical structure of the two conjugated dienes formed during the incubation period in more detail we prepared these compounds by RP-HPLC and further analyzed them by NP-HPLC. Here we found (upper inset to Fig. 10B) that the majority of the conjugated dienes coeluted with authentic standards of 12-HETE (early eluting diene) and 13-HODE(Z,E) (late eluting diene). Small amounts of other HODE isomers were also observed. Finally, we determined the enantiomer composition of the major conjugated dienes formed by tupALOX15a. Here (lower insets in Fig. 10B) we found for both, that 12-HETE and 13-HODE were predominantly the *S*-enantiomer. Only small amounts of the corresponding *R*-isomers were detected. Taken together, these data indicate that tupALOX15a is capable of oxidizing membrane bound polyenoic fatty acids and that the stereochemistry of the oxygenation reaction was tightly controlled by the enzyme. When we calculated the OH-PUFA/

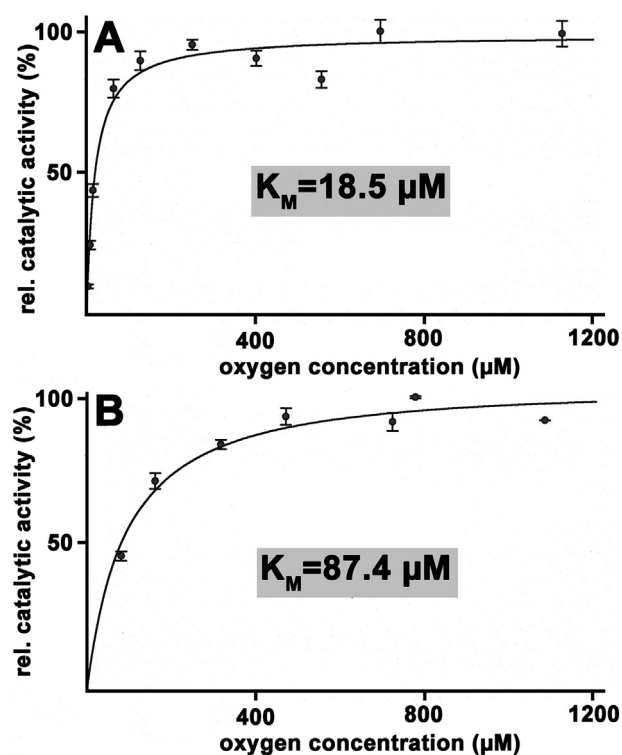


**Fig. 5.** Oxygen affinity of tree shrew ALOX15 isoforms. Tree shrew ALOX15 isoforms (tupALOX15a and tupALOX15c) were expressed in *E. coli* and activity assays were carried out at different oxygen concentrations as described in the Mat + Meth section. The highest reaction rate measured for either enzyme was set 100%. Regression curves were constructed with the Sigma-plot program. Activity assays at each oxygen concentration were carried out in duplicate and means and standard errors are given.

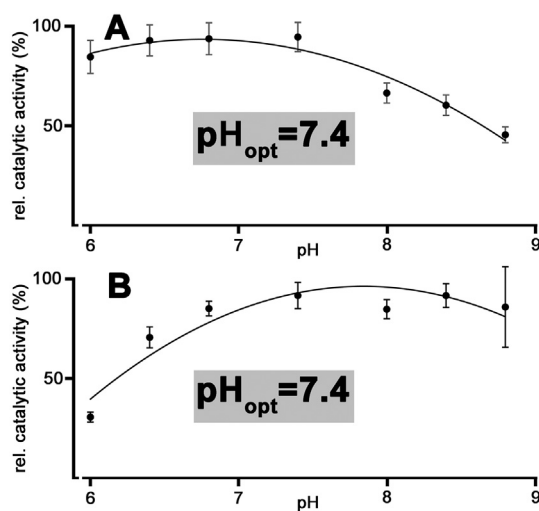


**Fig. 6.** pH-profiles of arachidonic acid oxygenation by the two tree shrew ALOX15 isoforms. Tree shrew ALOX15 isoforms (tupALOX15a and tupALOX15c) were expressed in *E. coli* and activity assays were carried out at different pH values using arachidonic acid (80 µM) as substrate. The buffer system consisted of equal volumes of 10 mM borate buffer and 10 mM phosphate buffer and the final pH was adjusted by the addition of 2 M HCl or 2 M NaOH. The highest oxygenase activity measured for either enzyme was set 100%. Regression curves were constructed with MS Excel. Activity assays were carried out in duplicate. Means and standard errors are given.

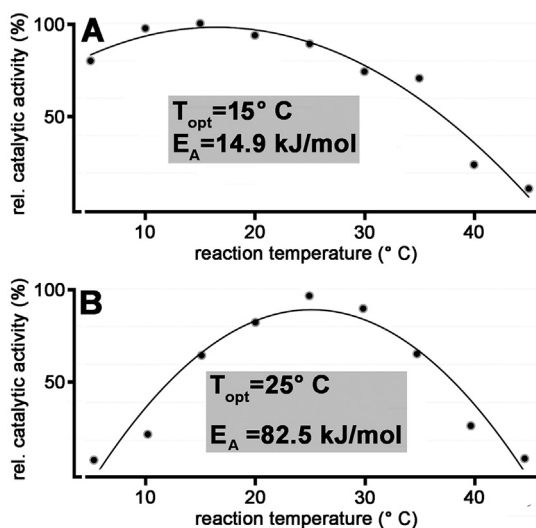


Fig. 7. Temperature profiles of arachidonic acid oxygenation by the two tree shrew ALOX15 isoforms. Tree shrew ALOX15 isoforms (tupALOX15a and tupALOX15c) were expressed in *E. coli* and activity assays were carried out at different temperatures using arachidonic acid (80  $\mu$ M) as substrate. The highest oxygenase activity measured for either enzyme was set 100%. Regression curves were constructed with MS Excel. For each temperature, a single activity assay was carried out.

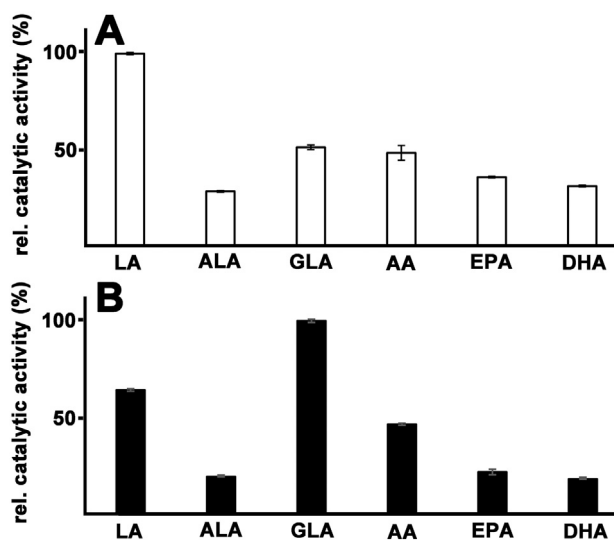
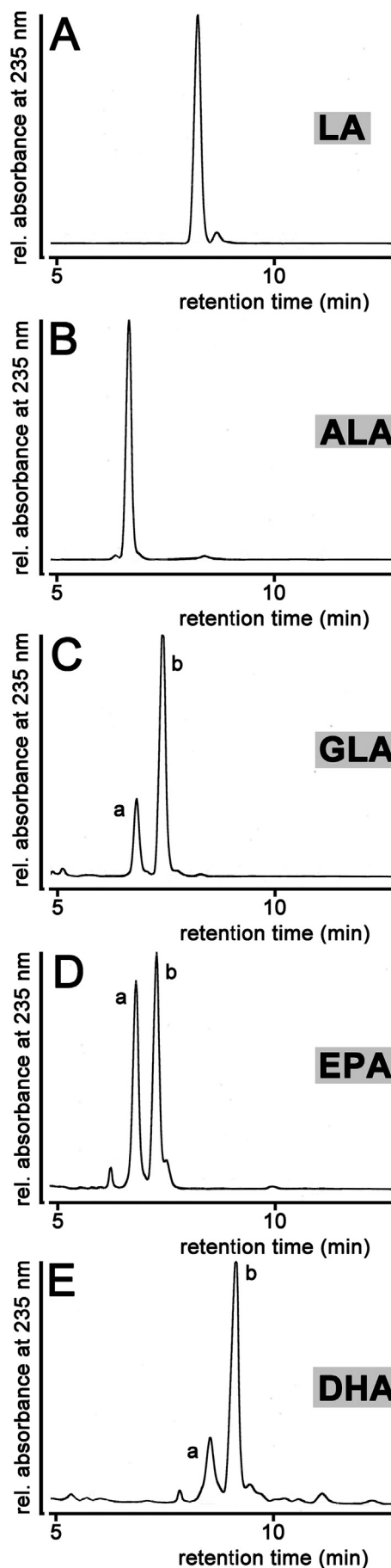


Fig. 8. Substrate specificity of the two tree shrew ALOX15 isoforms. Tree shrew ALOX15 isoforms (tupALOX15a and tupALOX15c) were expressed in *E. coli* and activity assays were carried out using different polyenoic fatty acids (80  $\mu$ M) as substrate. The reaction rates of the most suitable substrates (LA for tupALOX15a, GLA for tupALOX15c) were set 100%. Activity assays were carried out in duplicate and means and standard errors are given.

PUFA ratio, which constitutes a suitable measure for the degree of oxygenation of the membrane lipids, we found that 5.6% of the major polyenoic fatty acids (AA + LA) were present as hydroxylated derivatives. In the non-enzyme control incubation, this value was lower than 0.01%.

Almost identical reaction products were analyzed when tupALOX15c was used as catalyst (data not shown). However, for this enzyme we quantified a lower OH-PUFA/PUFA ratio (1.6%). It should be kept in mind that tupALOX15c is expressed at lower levels than tupALOX15a (Fig. 2B). Since identical volumes of lysis supernatants (50  $\mu$ L) were employed for the membrane oxygenase assays, the reduced membrane oxygenase activity of tupALOX15c is plausible.



(caption on next page)

**Fig. 9.** RP-HPLC of the conjugated dienes formed during the oxygenation reaction of different fatty acid substrates by *tup*ALOX15a. Tree shrew ALOX15a was expressed in *E. coli* and activity assays were carried out using different polyenoic fatty acids (80  $\mu$ M) as substrate. The conjugated dienes formed during a 3 min incubation period were analyzed by RP-HPLC (see Mat+Meth section). The chemical structures of the different conjugated dienes were identified by GC/MS (Table 3). Almost identical product profiles were obtained for *tup*ALOX15c. Activity assays were carried out in duplicate for each fatty acid and a representative chromatogram is shown.

## 2.6. Mutagenesis studies on tree shrew ALOX15 orthologs

The reaction specificity of arachidonic acid oxygenation by ALOX15 orthologs depends on the geometry of three different amino acids at the active site of the enzymes. The Triad Concept suggests that the bulkiness of the side chains aligning with Phe353 (Borngraber 1 determinant), Met418/Ile419 (Sloane determinants) and Ile593 (Borngraber 2 determinant) of rabbit ALOX15 is decisive for the specificity of arachidonic acid oxygenation. If a small amino acid (Leu, Ala) is located at Phe353 the enzyme is 12-lipoxygenating as it is the case for mouse and rat ALOX15. If a bulky Phe is located at this position the geometry of the amino acids located at positions 418/419 become decisive. For 15-lipoxygenating ALOX15 isoforms (human, chimpanzees, orangutan) bulky residues such as Ile or Met are located at these positions. In contrast, in 12-lipoxygenating ALOX15 orthologs (macaque, baboons, pigs) small amino acids (Val, Ala) are located there. For the two tree shrew ALOX isoforms, Phe353 of human ALOX15 aligns with a bulky Phe (Fig. S1). In contrast, Ile418/Met419 motif of human ALOX15 aligns with the Val/Val motif (two small residues). On the basis to the Triad Concept, a 12-lipoxygenating activity can be predicted and analysis of the reaction products (Fig. 3) confirmed this prediction. To explore whether the major triad determinants of *tup*ALOX15a and *tup*ALOX15c physically interact with each other we first mutated the Val418/Val419 motif of *tup*ALOX15a and *tup*ALOX15c to the residues present at these positions in the 15-lipoxygenating human ALOX15 as described [28]. Here we observed a gradual increase in the share of 15-HETE for the two single mutants Val418Ile and Val419Met (Table 4). Consistent with the Triad Concept the double mutant Val418Ile + Val419Met was almost completely 15-lipoxygenating (Table 4). Finally, we mutated in the 15-lipoxygenating double mutant Val418Ile + Val419Met the Phe353 residue to less bulky Ala/Leu and observed dominantly 12-lipoxygenating activity (Table 4). Thus, as predicted by the Triad Concept Phe353Ala exchange reverses the alterations in the positional specificity induced by Val418Ile + Val419Met double mutation. These data indicate that the Triad Concept is fully applicable for the two tree shrew ALOX15 isoforms and that the triad determinants of the reaction specificity physically interact with each other.

## 2.7. Tissue specific expression of tree shrew ALOX15 isoforms

We further explored the tissue specific expression of *tup*ALOX15a and *tup*ALOX15c. For this purpose, total RNA was extracted from the major organs of three tree shrew individuals and reverse transcriptase (RT)-PCR was carried out with a primer combination, which did not differentiate between *tup*ALOX15a and *tup*ALOX15c. Here we found that ALOX15 transcripts were expressed at rather high levels in the brain (Fig. 10). These data were rather surprising since in mouse brain ALOX15 orthologs are only expressed at very low levels. In addition, we also detected low-level expression of the *tup*ALOX15 transcripts in lung, liver and spleen, but not in kidney and heart. In addition to the specific *tup*ALOX15 amplification products, non-specific bands appeared in PCR. We sequenced all major non-specific bands with a size larger than 295 bp, none of the obtained sequences could be matched to the tree shrew genome. Since the primer pair we used for amplification of the *tup*ALOX15 transcripts did not distinguish between the different

**Table 3** Identification of the oxygenation products formed from different polyenoic fatty acids by *tup*ALOX15a and *tup*ALOX15c. Activity assays were carried out for *tup*ALOX15a and *tup*ALOX15c using different polyenoic fatty acids (100  $\mu$ M final concentration) as substrate. The conjugated dienes formed (see Fig. 9) were isolated and analyzed by GC-MS as described in the Mat + Meth section. Products (a, b) are labeled as indicated in Fig. 9. For calculation of the relative reaction rates conjugated diene formation of the best substrate (C18: $\Delta$ 6,9,12 for *tup*ALOX15a and C18: $\Delta$ 6,9,12 for *tup*ALOX15c; given in bold face) was set 100%. Activity assays were carried out in duplicate and means  $\pm$  standard errors are given.

Substrate fatty acid	Rel. reaction rates (%)		Product	ALOX15a	ALOX15c	Oxygenation site	Informative ions in MS; m/z (rel. abundance)
	ALOX15a	ALOX15c					
C18: $\Delta$ 9,12 ( $\omega$ -6)	99.6 $\pm$ 0.2	63.6 $\pm$ 0.6	a	> 95%	> 95%	n-6 (C <sub>13</sub> )	73 (100), 173 (10.7), 369 (7.8, $\alpha$ -cleavage), 425 (0.7, M <sup>+</sup> -15), 440 (1.7, M <sup>+</sup> )
C18: $\Delta$ 9,12,15 ( $\omega$ -3)	28.3 $\pm$ 0.2	18.7 $\pm$ 0.2	a	> 95%	> 95%	n-6 (C <sub>13</sub> )	73 (100), 171(12.4), 369 (70.9, $\alpha$ -cleavage), 423 (1.9, M <sup>+</sup> -15), 438 (0.3, M <sup>+</sup> )
C18: $\Delta$ 6,9,12 ( $\omega$ -6)	51.1 $\pm$ 1.2	<b>99.4 <math>\pm</math> 0.8</b>	a	23%	37%	n-6 (C <sub>13</sub> )	73 (100), 173 (9.3, $\alpha$ -cleavage), 367 (1.3), 423 (0.6, M <sup>+</sup> -15), 438 (0.2, M <sup>+</sup> )
C20: $\Delta$ 5,8,11,14,17 ( $\omega$ -3)	35.6 $\pm$ 0.2	21.2 $\pm$ 1.4	b	77%	63%	n-9 (C <sub>10</sub> )	73 (100), 327 (79.2, $\alpha$ -cleavage), 423 (4.7, M <sup>+</sup> -15), 438 (2.6, M <sup>+</sup> )
C22: $\Delta$ 4,7,10,13,16,19 ( $\omega$ -3)	31.0 $\pm$ 0.2	17.5 $\pm$ 0.1	b	44%	55%	n-6 (C <sub>15</sub> )	73 (100), 171 (35.1, $\alpha$ -cleavage), 393 (3.3), 447 (2.1, M <sup>+</sup> -15), 462 (1.0, M <sup>+</sup> )
				56%	45%	n-9 (C <sub>12</sub> )	73 (100), 211 (8.5, $\alpha$ -cleavage), 353 (9.0), 447 (2.1, M <sup>+</sup> -15), 462 M <sup>+</sup>
				25%	24%	n-6 (C <sub>17</sub> )	73 (100), 171 (59.9, $\alpha$ -cleavage), 473 (4.1, M <sup>+</sup> -15), 488 (5.7, M <sup>+</sup> )
			b	75%	76%	n-9 (C <sub>14</sub> )	73 (100), 211 (14.5, $\alpha$ -cleavage), 379 (5.8), 473 (2.2, M <sup>+</sup> -15), 488 (1.8, M <sup>+</sup> )

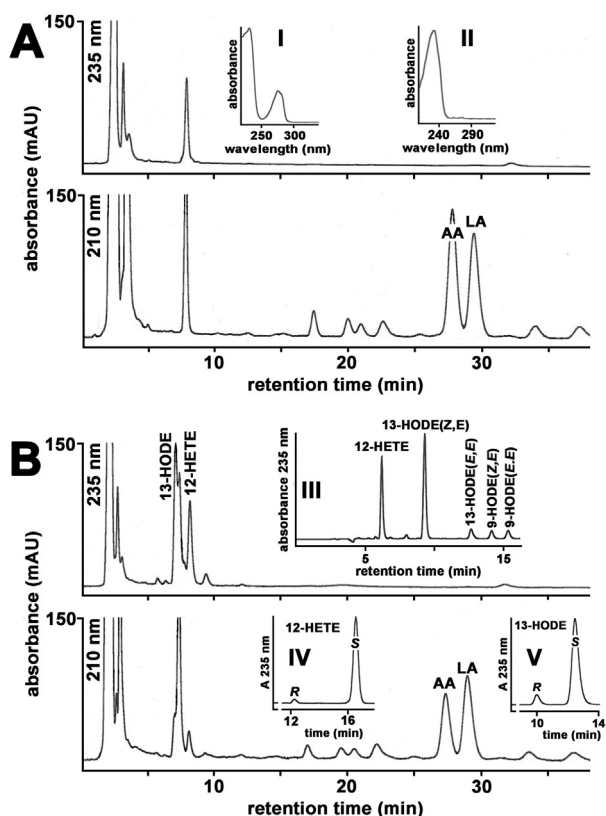


Fig. 10. Membrane oxygenase of tree shrew ALOX15 isoforms.

tupALOX15a was expressed in *E. coli* and membrane oxygenase assays were carried out as described in Mat + Meth. After hydrolysis of the lipid extracts the formation of conjugated dienes was quantified by RP-HPLC. The major conjugated dienes formed were prepared by RP-HPLC and further analyzed by NP- and CP-HPLC. A) RP-HPLC of a non-enzyme control. Left inset: UV-spectrum of the unknown compound(s) eluting with a retention time of about 8 min. Right inset: UV-spectrum of the conjugated diene coeluting with an authentic standard of 13-HODE. The conjugated diene coeluting with an authentic standard of 12-HETE exhibited a similar UV-spectrum. B) RP-HPLC chromatogram of conjugated dienes formed by tupALOX15a. Upper inset: NP-HPLC of RP-HPLC purified conjugated dienes. Lower left inset: CP-HPLC of NP-HPLC purified 13-HODE formed by tupALOX15a during the membrane oxygenation assay. Lower right inset: CP-HPLC of NP-HPLC purified 12-HETE formed by tupALOX15a during membrane oxygenation assay. Membrane oxygenase activity assays were carried out in duplicate and representative RP-HPLC chromatograms are shown. For NP- and CP-HPLC, the products of the different assays were pooled.

Table 4

Reaction specificity of tupALOX15 mutants. Wildtype and mutant tupALOX15 isoform variants were expressed in *E. coli* (see Materials and Methods) and the reaction specificity of the enzymes was determined analyzing the major oxygenation products by RP-HPLC after a 3 min incubation period of the enzymes with arachidonic acid. The one letter code of amino acids is used. The sum of the major oxygenation products (12-HETE + 15-HETE) was set 100%.

Enzyme	tupALOX15a		tupALOX15c	
	12-HETE (%)	15-HETE (%)	12-HETE (%)	15-HETE (%)
Wildtype	93.3	6.7	92.3	7.7
V418I	23.1	76.9	21.5	78.5
V419M	75.9	24.1	54.6	45.5
V418I + V419M	5.1	94.9	5.9	94.1
V418I + V419M + F353A	92.9	7.1	89.6	10.2
V418I + V419M + F353L	77.6	22.4	16.9	83.1

tupALOX15 transcripts, we sequenced the amplification products obtained by RT-PCR (295 bp band in Fig. 10) using the Taq-amplified sequencing technique. For this purpose the amplification products were cloned and 20 well-separated clones were independently sequenced. The results indicated that in the brain the tupALOX15a gene was expressed at much higher levels than tupALOX15c gene (tupALOX15a vs. tupALOX15c ratio of 8:1). In contrast, tupALOX15c was the major ALOX15-isoform expressed in the lungs and in the spleen. In fact, of the 20 clones selected for the lung amplification product 19 clones did represent tupALOX15c transcripts and one clone represented a tupALOX15d message. No clones representing tupALOX15a transcripts were among the selected bacterial colonies. In spleen tissue, all randomly selected bacterial colonies represented tupALOX15c transcripts. Taken together, these data indicate that tupALOX15a and tupALOX15c genes are differentially expressed in different tissues of the Chinese tree shrew. The other two tupALOX15 genes (tupALOX15b, tupALOX15d) were hardly expressed in brain, lung and spleen.

### 3. Discussion

#### 3.1. Tree shrew as an alternative model for human diseases

The tree shrew is a highly developed squirrel-like mammal, which is widely distributed in Southeast Asia. This species has a number of unique characteristics, which makes it meaningful to use it as experimental animal [18]. The availability of the annotated genome sequence [21,22] and the public genome database ([www.treeshrewdb.org](http://www.treeshrewdb.org)) offers a solid basis for functional studies on selected proteins and for the creation of whole animal models of human diseases. Most importantly, in mammalian evolution the tree shrew is more closely related to humans when compared with the frequently employed laboratory animals such as mice and rats (Fig. 1). A large number of functional studies on the genes involved in immune and nervous systems have provided deep insights into the biology of this animal [45–47]. The extensive characterization of key factors and signalling pathways in the immune and nervous systems has shown that tree shrews possess both conserved and unique features relative to primates [19]. Thus, the tree shrew has been successfully used to create animal models for myopia, depression, breast cancer, alcohol-induced or non-alcoholic fatty liver diseases, herpes simplex virus type 1 (HSV-1) and hepatitis C virus (HCV) infections [17,19,24], to name a few. Although the recent successful genetic manipulation of the tree shrew [48] has opened a new avenue for a more frequent usage of this animal in basic biomedical research, our knowledge on mouse genetics is still more comprehensive when compared with the tree shrew. However, employing the Crispr/Cas technology [49], it will be possible to manipulate the tree shrew genome in any wanted way and thus, this animal will be increasingly employed in the future to explore the mechanistic basis of different human diseases [19].

#### 3.2. Comparison of tree shrew ALOX15 isoforms with orthologs of other mammals

Most mammalian genomes sequenced so far including the human and the mouse genome involve a single copy of the ALOX15 gene. The enzymes (ALOX-isoforms) encoded by these single copy genes share a high degree (80–90%) of amino acid conservation [50], when different mammals are compared with each other. Rabbit [51] and porcine [52] ALOX15 have been purified from natural sources and a number of other mammalian ALOX15 orthologs have been expressed as recombinant enzymes in pro- and eukaryotic systems [30,31,53–55]. Unfortunately, for the time being there has not been any information on the functional characteristics of the ALOX15 pathway in *Scandentia* and this gap of knowledge was at least partially filled by the present study.

Consistent with other mammalian ALOX15 orthologs [3,56,57], the two tupALOX15 isoforms characterized in this study exhibit broad

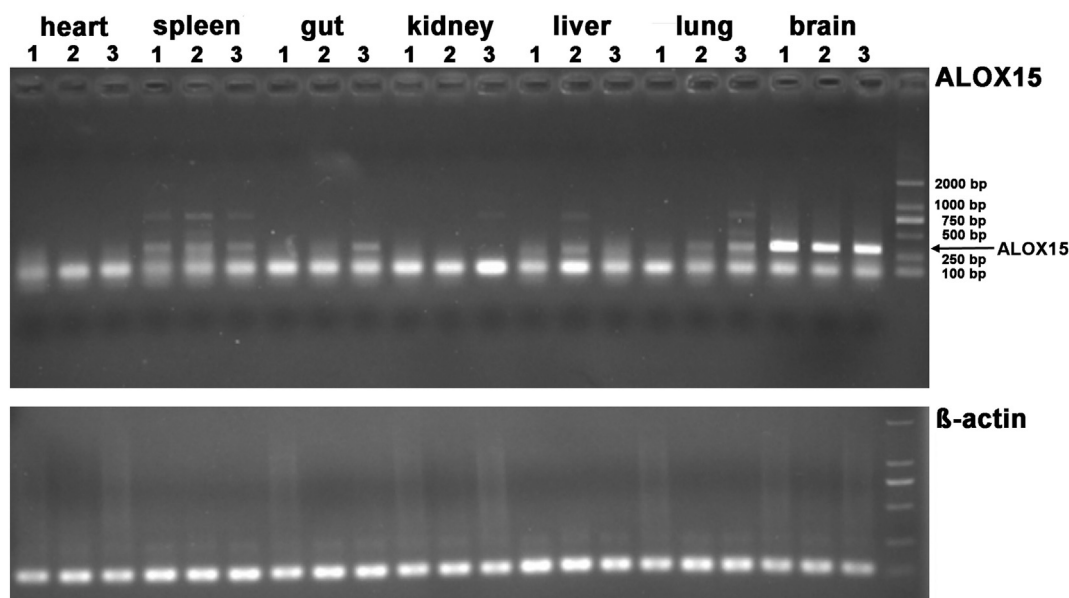


**Fig. 11.** Tissue specific expression of tree shrew ALOX15 transcripts. Total RNA was extracted from seven different tissues (each from three healthy adult tree shrews) and tissue-specific expression of *tup*ALOX15 isoforms was tested at the mRNA level by reverse transcriptase-PCR (see Mat + Meth section for mechanistic details and primer sequences). The arrow indicates the molecular weight of the expected specific amplification product with a size of 295 bp.

substrate specificities. They oxygenate most naturally occurring polyenoic fatty acids with similar reaction rates (Table 4). However, there are subtle differences between the two isoforms. For *tup*ALOX15a, linoleic acid is the preferred free fatty acid. In contrast, for *tup*ALOX15c GLA is optimal. These data suggested that the substrate fatty acids are differently aligned at the active site of the two isoforms so that the rate-limiting step of the overall reaction is catalyzed with different efficiency.

Tree shrew ALOX15 isoforms are capable of oxygenating membrane ester lipids (Fig. 10). Such membrane oxygenase activity was first reported for native rabbit ALOX15 [42] and has later been confirmed for recombinant human [58], recombinant rat [53] and native porcine [59] ALOX15 orthologs. Since a rather specific pattern of oxygenation products is formed (Fig. 10) one can conclude that the oxygenation of the membrane lipids is strongly enzyme controlled. However, the membrane oxygenase activity is almost one order of magnitude less effective than the fatty acid oxygenase activity. In fact, when similar amounts of enzyme are used for the standard activity assays much more conjugated dienes are formed in the fatty acid oxygenase tests. This has also been reported for other ALOX15 orthologs [60]. It should be stressed at this point that the standard activity assays for fatty acid and biomembrane oxygenation are quite different and that the membrane proteins may inhibit substrate binding at the active site. Thus, the two catalytic activities should not directly be compared with each other unless suitable normalization procedures are applied.

### 3.3. The *tup*ALOX15 isoforms follow the Triad Concept and the Evolutionary Hypothesis of ALOX15 specificity

Mammalian ALOX15 orthologs can be classified in two different subgroups: i) arachidonic acid 12-lipoxygenating enzymes and ii) arachidonic acid 15-lipoxygenating enzymes. According to the Evolutionary Concept of mammalian ALOX15 specificity [27] the enzymes from mammals ranked higher in evolution than gibbons including recent [61] and extinct human subspecies [62,63] express arachidonic acid 15-lipoxygenating enzymes. In contrast, ALOX15 orthologs of mammals ranked lower than gibbons express 12-lipoxygenating orthologs [31,55,64,65]. There are rare exceptions [30,32] but most ALOX15 orthologs adhere to this concept. Since the tree shrew is ranked lower in evolution than gibbons the *tup*ALOX15 isoforms

should oxidize arachidonic acid predominantly at carbon 12 (12-HETE formation). Here we showed (Fig. 3) that arachidonic acid is mainly oxygenated to 12S-H(p)ETE and thus, our data indicate the applicability of the Evolutionary Concept for this mammalian species.

When we mutated the Sloane determinants (Val418 + Val419) of *tup*ALOX15a and *tup*ALOX15c, which are identical for the two iso-enzymes, to the more space-filling residues present at these positions in 15-lipoxygenating ALOX15 orthologs (Val418Ile, Val419Met, Val418Ile + Val419Met) we observed the expected alterations in the reaction specificity (Table 4). For all mutants a strong increase in the formation of 15-HETE was observed. In fact, the Val418Ile + Val419Met double mutant produced almost exclusively 15-HETE and these data indicate that these amino acid residues are important for the reaction specificity of this enzyme. In previous experiments similar mutagenesis strategies have been applied for different 12- and 15-lipoxygenating ALOX15 orthologs [31,33,53,66] including the human enzyme [67] and always similar alterations in the reaction specificity were observed. When we mutated in the Val418Ile + Val419Met double mutant Phe353 to a less space-filling residue (Phe353Ala, Phe353Leu), we reversed the alteration introduced in the reaction specificity by the Val418Ile + Val419Met double mutations. In fact, the Phe353Ala + Val418Ile + Val419Met triple mutant is a dominantly 12-lipoxygenating enzyme. These data indicate that all mammalian ALOX15 orthologs tested so far including the *tup*ALOX15 isoforms follow the Triad Concept [33,50].

### 3.4. Tissue specific expression pattern of *tup*ALOX15 isoforms

One of the most interesting findings of this study is that in tree shrew ALOX15 isoforms are highly expressed in the brain (Fig. 11). In this organ *tup*ALOX15a transcripts were dominant. In lungs and spleen we also detected *tup*ALOX15 transcripts but in these organs the *tup*ALOX15c gene was mainly expressed. The high cerebral expression levels of *tup*ALOX15a transcripts were rather surprising since in other mammals the brain is not a major site of ALOX15 expression. In fact, in mice the enzyme is virtually absent in normal brain [68]. However, after focal ischemia, expression of ALOX15 was increased in neurons and in vascular endothelial cells [69]. In this ischemia model significant leakage of plasmaproteins into the brain parenchyma was observed and this leakage was significantly reduced in ALOX15 knockout mice. These

data suggested that ALOX15 may contribute to ischemic brain damage by detrimental effects on cerebral microvasculature [69]. Similar effects were observed in different murine cerebral ischemia models [69–73] but also in human ischemic brain diseases. For instance, in periventricular leukomalacia, which frequently develops in human newborns as a consequence of perinatal hypoxia, expression of ALOX15 is strongly upregulated in activated oligodendrocytes [74]. These data suggest that ALOX15 constitutes a destructive enzyme, which may play a major role in the secondary degradation processes induced by cerebral ischemia. On the basis of this idea ALOX15 inhibitors have been suggested as future anti-stroke medication [70,75,76]. In the tree shrew, abundant ALOX15 expression was already seen in normal brain (Fig. 11). Unfortunately, for the time being we do not know yet, which cell type is the major source for *tup*ALOX15 and whether expression is particularly high in specific parts of the brain. Moreover, it remains unclear whether this overexpression can also be detected on the protein and/or the activity level. The ALOX15 [77,78] has been proposed as emerging therapeutic target for Alzheimer's disease (AD) and tree shrew possesses the genetic features for being used as a viable model for AD [79]. It would be rewarding to test the potential relationship between the genomic multiplicity of the ALOX15 genes and AD risk by using this animal. Finally, if ALOX15 is detrimental as it appears to be the case in mice and humans there must be mechanisms in tree shrews that prevent the detrimental effects under normal conditions. Identification of such protective mechanisms might be helpful for the development of innovative strategies of anti-stroke therapy in humans.

#### 4. Materials and methods

##### 4.1. Chemicals

All chemicals used for this study were obtained from the following sources: acetic acid from Carl Roth GmbH (Karlsruhe, Germany); sodium borohydride from Life Technologies, Inc. (Eggenstein, Germany); antibiotics and isopropyl- $\beta$ -thiogalactopyranoside (IPTG) from Carl Roth GmbH (Karlsruhe, Germany), restriction enzymes from Thermo Fisher Scientific-Fermentas (Schwerte, Germany); the *E. coli* strain Rosetta2 DE3 pLysS from Novagen (Merck-Millipore, Darmstadt, Germany) and *E. coli* strain XL-1 from Stratagene (La Jolla, USA). Oligonucleotide synthesis was performed at BioTez Berlin Buch GmbH (Berlin, Germany). Nucleic acid sequencing was carried out at Eurofins MWG Operon (Ebersberg, Germany). HPLC grade methanol, acetonitrile and water were from Fisher Scientific. Authentic HPLC standards of HETE-isomers [15(S/R)-HETE, 15(S)-HETE, 12(S/R)-HETE, 12(S)-HETE, 5(S)-HETE] and the polyenoic fatty acids used as ALOX substrates, such as linoleic acid (LA), alpha-linolenic acid (ALA), gamma-linolenic acid (GLA), arachidonic acid (AA), eicosapentaenoic acid (EPA) and docosahexaenoic acid (DHA) were purchased from Cayman Chem. [distributed by Biomol (Hamburg, Germany)].

##### 4.2. Database searches and sequence alignments

The protein sequence of human ALOX15 gene was aligned against the Chinese tree shrew genome using tBlastn (<https://blast.ncbi.nlm.nih.gov/Blast.cgi>). Best hit regions of each gene with 5 Kb flanking sequence were selected and re-aligned with the corresponding human ALOX15 protein sequence using the GeneWise program [80]. Using this methodology, we identified four copies of ALOX15 gene (*tup*ALOX15a, *tup*ALOX15b, *tup*ALOX15c, *tup*ALOX15d) in the Chinese tree shrew genome [22,81], which was retrieved from the tree shrew database ([www.treeshrewdb.org](http://www.treeshrewdb.org)).

##### 4.3. Cloning of tree shrew ALOX15 mRNAs

To identify ALOX15 gene copies in the tree shrew genome we searched the tree shrew genome database ([www.treeshrewdb.org](http://www.treeshrewdb.org)) for

ALOX15 sequences and obtained four hits. As concluded from their nucleotide sequences these genes encode for four structurally different ALOX15 isoforms. To test the functionality of the corresponding enzymes we extracted the cDNAs from the genomic sequence, optimized the coding regions for prokaryotic expression and had them chemically synthesized (Biocat, Heidelberg, Germany). For convenient subcloning a *SalI* restriction site was introduced immediately upstream of the starting ATG of the his-tag fusion construct and a *HindIII* site was included immediately downstream of the stop codon. To subclone the coding region into a prokaryotic expression vector it was excised from the synthesizing vector (pUC57) and cloned into the expression plasmid pET28b (Novagen/Merck, Darmstadt, Germany). The recombinant expression plasmids were tested for the presence of the ALOX15-insert by digestion with *SalI* and *HindIII* and finally the constructs were sequenced for validation.

##### 4.4. Bacterial expression of tree shrew ALOX15 isoforms

After subcloning of the coding regions of the *tup*ALOX15 cDNAs into the bacterial expression plasmids the enzymes were expressed as described previously [30]. In brief, competent bacteria (Rosetta 2 DE3 pLysS) were transformed with 100 ng of the recombinant expression plasmids and the cells were grown overnight on kanamycin/chloramphenicol containing agar plates. Four well-separated bacterial clones were selected and 1 mL bacterial liquid cultures (LB medium with 50  $\mu$ g/mL kanamycin/35  $\mu$ g/mL chloramphenicol) were grown at 37 °C. This pre-culture was checked for optical density after 6 h and appropriate amounts of the pre-culture were added to a 50 mL main culture to reach an OD<sub>600</sub> between 0.10 and 0.15. The culture medium (glucose-free MSM with added trace elements) was supplemented with 40 g/L dextrin, 0.24 g/L tryptone/peptone and 0.48 g/L yeast extract. Before starting the incubation, antibiotics as well as 100  $\mu$ L 1:20 diluted antifoam 204 (Sigma, Deisenhofen, Germany) and 50  $\mu$ L Glycoamylase from *Aspergillus niger* (Amylase AG 300 L, Novozymes, Bagsværd, Denmark) were added and the main cultures were grown overnight at 30 °C and continuously shaken at 250 rpm in Ultra Yield flasks (Thomson Instrument Company, Oceanside, USA). After checking the OD<sub>600</sub> (should be > 5), expression of the recombinant enzyme was induced by addition of 1 mM (final concentration) IPTG and 60 mg Tryptone/Peptone, 120 mg yeast extract and 75–100  $\mu$ L Glycoamylase were added. The cultures were then incubated at 22 °C for 24 h at 230–250 rpm agitation. After the culturing period, the bacteria were harvested by centrifugation and the resulting pellet was reconstituted in a total volume of 5 mL PBS. Bacteria were lysed by sonication [digital sonifier, W-250D Microtip Max 50% Amp, Model 102C (CE); Branson Ultrasonic, Fürth, Germany], cell debris was spun down (15 min, 15,000  $\times$ g, 4 °C) and the lysate supernatants were employed as enzyme source for functional characterization.

To quantify the ALOX15 content in the bacterial lysate supernatants we carried out quantitative immunoblotting employing a specific anti-his-tag antibody as probe. This antibody specifically recognizes the N-terminal hexa-his-tag tail of the expressed recombinant proteins and thus, the intensity of the immunoreactive protein band represents the amount of the recombinant ALOX15 protein. To calibrate the intensity scale of the immunoblots we loaded defined amounts of pure recombinant ALOX15 of *M. fulvus*, which was also expressed as hexa-his tag fusion protein. Since analyses were carried out under strongly denaturing conditions, which completely unfolds the recombinant proteins, the immunoreactivity of the antibody with the hexa-his-tag tail of tupaia ALOX15 isoforms and with the corresponding motif of *M. fulvus* ALOX should be comparable. However, it cannot be completely excluded that the ALOX-share of the fusion protein does not impact the immunoreactivity. The likelihood of such an impact is rather low since under our analytical conditions the immunological epitope (the hexa-his-tag tail) should be freely accessible for the antibody.

#### 4.5. SDS-PAGE and Western blot

For immunoblotting 6  $\mu$ L lysate supernatant (100  $\mu$ g protein) were applied to the MagneHis Protein Purification System (Promega Corp., Madison, USA). In Detail, 74  $\mu$ L sterile water, 6  $\mu$ L lysate supernatant, 10  $\mu$ L  $10\times$  FastBreak and 15  $\mu$ L MagneHis-Beads were mixed, incubated for 30 min at 25 °C and vigorous shaking at 1100 rpm. The supernatant was discarded, the protein loaded beads were reconstituted in 20  $\mu$ L of two-fold concentrated sample buffer and the empty beads were spun down. The supernatant containing the eluted proteins was used for SDS-PAGE. Electrophoresis was carried out on a 7.5% polyacrylamide gel in a Bio-Rad electrophoretic chamber with ProSieve Ex running buffer (Lonza Group Ltd., Basel, Switzerland) for 25 min at 200 V. Proteins were transferred to a Protran BA 85 Membrane (Carl Roth GmbH, Karlsruhe, Germany) using rapid transfer buffer (VWR International GmbH, Darmstadt, Germany) for 22 min at 400 mA. The membrane was blocked with 5% blotting grade blocker (Bio-Rad Laboratories GmbH, Munich, Germany) in PBS for 30 min at room temperature. The membrane was washed in PBS/TWEEN and afterwards incubated with an anti-His-HRP antibody (Miltenyi Biotec GmbH, Bergisch Gladbach, Germany) for 1–2 h at room temperature. After repeated washing, the membrane was developed using the SERVALight Polaris CL HRP WB Substrate Kit for 5 min at room temperature. Chemiluminescence was detected at a FUJIFILM Luminescent Image Analyzer LAS-1000plus & Intelligent Dark Box II. The protein amount was quantified relative to known amounts (250 and 500 ng) of purified *M. fulvus* ALOX protein using ImageJ software.

#### 4.6. Activity assays

To assay the catalytic activity of the recombinant enzyme preparations variable amounts of the bacterial lysis supernatants were added to 0.5 mL of PBS containing fatty acid substrates at different concentrations. After 3–10 min of incubation, the hydroperoxy fatty acids formed were reduced to the corresponding alcohols by the addition of 1 mg of solid sodium borohydride. After 5 min, the reaction mixture was acidified with 45  $\mu$ L of concentrated acetic acid and proteins were precipitated by the addition of 0.455 mL of acetonitrile. The samples were placed on ice for 10 min, precipitated proteins were removed by centrifugation and aliquots of the protein-free supernatants (50–300  $\mu$ L) were injected to RP-HPLC analyses. For this purpose, a Shimadzu instrument equipped with a Hewlett Packard diode array detector 1040 A was employed and the metabolites were separated on a Nucleodur C18 Gravity column (Macherey-Nagel, Düren, Germany; 250  $\times$  4 mm, 5  $\mu$ m particle size), which was coupled with a guard column (8  $\times$  4 mm, 5  $\mu$ m particle size). The solvent system consisted of acetonitrile:water:acetic acid (70:30:0.1, by vol) and a flow rate of 1 mL/min was maintained throughout the run. The chromatographic scale was calibrated by injecting known amounts of 15-HETE, arachidonic acid and linoleic acid (six point calibration curves for each metabolite).

To explore the oxygen affinity of the tree shrew ALOX15 isoforms, we mixed different amounts of anaerobic PBS containing 80  $\mu$ M arachidonic acid (flushed with argon for 15 min) with hyperoxic PBS also containing 80  $\mu$ M arachidonic acid (flushed with oxygen gas for 15 min) in a gas-tight reaction chamber (chamber volume of 1.1 mL), which was previously filled with argon. First, we added the anaerobic reaction solution into the chamber via a capillary inlet port. Next, a defined volume of the hyperoxic solution was added so that the entire reaction chamber was filled with fluid. From the volume ratio of anaerobic and hyperoxic solution we calculated the oxygen concentration in the reaction chamber. Finally, we started the reaction by the addition of small amounts (5–25  $\mu$ L) of partially anaerobized enzyme preparation and assayed the amounts of reaction products formed during a 3 min incubation period by RP-HPLC.

#### 4.7. Reaction product identification

Compounds absorbing at 235 nm, which elute in RP-HPLC in the hydroxy fatty acid region (retention time between 7 and 12 min), were prepared and further analyzed by normal- (NP-HPLC) and/or chiral-phase HPLC (CP-HPLC). Normal phase HPLC was performed on a Nucleosil 100–5 column (250  $\times$  4.6 mm, 5  $\mu$ m particle size) with the solvent system n-hexane/2-propanol/acetic acid (100/2/0.1, by volume) and a flow rate of 1 mL/min. Retention times of 13-HODE, 9-HODE, 12-HETE, 15-HETE, 8-HETE and 5-HETE were determined by injecting authentic standards. 13-HODE enantiomers were separated as free acids on a Chiralcel OD column (4.6  $\times$  250 mm, 5  $\mu$ m particle size, Daicel Chem., Osaka, Japan) using a solvent system consisting of hexane/2-propanol/acetic acid (100/5/0.1, by vol.) at a flow rate of 1 mL/min. Free 12-HETE enantiomers were resolved on a Chiralpak AD-H column (Daicel Corp., Osaka, Japan) with a solvent system consisting of n-hexane/methanol/ethanol/acetic acid (96/3:1:0.1, by vol, 1 mL/min).

#### 4.8. GC/MS analysis of the reaction products

To identify the chemical structure of the major oxygenation products of the different polyenoic fatty acids, the dominant conjugated dienes were prepared by RP-HPLC, silylated using BSTFA and further analyzed by GC-MS on an Agilent 6897 gas chromatograph coupled with an Agilent 5973 N mass selective detector and equipped with a HP-5 ms column (25 m  $\times$  0.25 mm, coating thickness 0.25  $\mu$ m) with a deactivated fused silica guard column (5 m  $\times$  0.32 mm). Helium was used as carrier gas at a total flow rate of 1.1 mL/min. The source temperatures were set at 230 °C. To avoid sample degradation in the injector the derivatized oxygenation products (1  $\mu$ L) were injected using a cool on-column inlet and then the analytes were eluted using the following temperature program: isothermally at 70 °C for 3 min and then from 70 °C to 270 °C at a rate of 30 °C/min.

#### 4.9. Membrane oxygenase activity

To test the membrane oxygenase activity of the two tree shrew ALOX15 isoforms (tupALOX15a, tupALOX15c) we incubated different volumes (50–150  $\mu$ L) of the bacterial lysis supernatants in 0.5 mL PBS with sub-mitochondrial particles (1.4 mg/mL final membrane protein concentration) as model membranes. These membrane preparations have previously been identified as the most suitable substrates for rabbit ALOX15 [42]. After a 5 min incubation period the reaction was terminated by the addition of NaBH<sub>4</sub> and then the sample was acidified with 35  $\mu$ L of acetic acid. Total lipids were extracted [82], ester lipids were hydrolyzed under alkaline conditions and aliquots of the hydrolysate were injected to RP-HPLC. The chromatograms were followed at 235 nm (detection of conjugated dienes formed during the incubation period) and at 210 nm (detection of non-oxidized polyenoic fatty acids). From the peak areas of the major polyenoic fatty acids (LA + AA) and the conjugated dienes formed during the incubation period the hydroxy fatty acid/PUFA ratio was calculated, which constitutes a suitable measure to quantify the degree of oxygenation of the membrane lipids [43].

#### 4.10. Tissue specific expression of tupALOX15 isoforms

Total RNA was extracted from different tissues and the cDNAs were prepared as described previously [83]. PCR was performed by using the 2  $\times$  TSINGKE Master Mix (green) (TsingKe Company, Beijing, China; lot # TSE001) supplemented with the primer pair Tup+m\_845up TGGATGGGATCAAGGCCAATGT/Tup+m\_1139do AGGCACCTCATGG TGGCCAC, which could amplify all four isoforms of tupALOX15. The amplification product had a molecular weight of 295 bp and we employed the  $\beta$ -actin as reference gene for normalization purpose [45,47].

The PCR reaction was carried out in a volume of 20  $\mu$ L solution containing 1  $\mu$ M each primer, 1  $\mu$ L cDNA template, and 10  $\mu$ L  $2 \times$  TSINGKE Master Mix. The cycling condition was composed of an initial denaturation cycle at 98 °C for 3 min, 30 cycles of 15 s at 98 °C, 30 s at 60 °C, and a final extension step at 72 °C for 15 s. We performed TA-cloning sequencing for the PCR products from the brain, lung and spleen tissues, and randomly sequenced 20 positive clones using the M13 forward primer of the vector.

Supplementary data to this article can be found online at <https://doi.org/10.1016/j.bbalip.2019.158550>.

### Acknowledgements and funding

This work was supported by grants from the Deutsche Forschungsgemeinschaft - DFG (KU961/13-1, KU961/14-1 to H.K., HE8295/1-1 to D.H.), Russian Foundation for Basic Research (19-54-12002 to I.I.) and National Natural Science Foundation of China (U1402224 to Y.-G. Y., 31970542 and 31601010 to Y.F.), Chinese Academy of Sciences (CAS zsys-02) and Yunnan Province (2018FB054 to Y.F.).

### Author contributions

M.S. and D.H. designed the expression vectors. M.S. and S.S. prepared the enzymes. M.S., H.K. and D.H. performed the activity assays and characterized the enzyme preparations. I.I. carried out GC-MS analyses of the reaction products. Y.F. analyzed the tree shrew genome, T.G. performed the tissue expression assay. H.K., D.H., Y.-G. Y. and M.S. designed the study and coordinated the experiments. H.K. and D.H. drafted the manuscript and all co-authors edited and commented it.

### Declaration of Competing Interest

The authors declare that they do not have any conflicts of interest with the content of this article.

### References

- [1] J.Z. Haeggstrom, C.D. Funk, Lipoxygenase and leukotriene pathways: biochemistry, biology, and roles in disease, *Chem. Rev.* 111 (10) (2011) 5866–5898.
- [2] H. Kuhn, S. Banthiya, K. van Leyen, Mammalian lipoxygenases and their biological relevance, *Biochim. Biophys. Acta* 1851 (4) (2015) 308–330.
- [3] M. Colakoglu, S. Tuncer, S. Banerjee, Emerging cellular functions of the lipid metabolizing enzyme 15-Lipoxygenase-1, *Cell Prolif.* 51 (5) (2018) e12472.
- [4] K. Mikulska-Ruminska, I. Shrivastava, J. Krieger, S. Zhang, H. Li, H. Bayir, et al., Characterization of differential dynamics, specificity, and allostery of lipoxygenase family members, *J Chem Inf Model* 59 (2019) 2496–2508.
- [5] T. Horn, S. Adel, R. Schumann, S. Sur, K.R. Kakularam, A. Polamarasetty, et al., Evolutionary aspects of lipoxygenases and genetic diversity of human leukotriene signaling, *Prog. Lipid Res.* 57 (2015) 13–39.
- [6] C. Wasternack, I. Feussner, The oxylipin pathways: biochemistry and function, *Annu. Rev. Plant Biol.* 69 (2018) 363–386.
- [7] M. Liu, T. Yokomizo, The role of leukotrienes in allergic diseases, *Allergol. Int.* 64 (1) (2015) 17–26.
- [8] A. Ryan, C. Godson, Lipoxins: regulators of resolution, *Curr. Opin. Pharmacol.* 10 (2) (2010) 166–172.
- [9] M. Spite, J. Claria, C.N. Serhan, Resolvins, specialized proresolving lipid mediators, and their potential roles in metabolic diseases, *Cell Metab.* 19 (1) (2014) 21–36.
- [10] C.R. Pace-Asciak, Pathophysiology of the hepxilins, *Biochim. Biophys. Acta* 1851 (4) (2015) 383–396.
- [11] C.D. Funk, X.S. Chen, E.N. Johnson, L. Zhao, Lipoxygenase genes and their targeted disruption, *Prostaglandins Other Lipid Mediat.* 68–69 (2002) 303–312.
- [12] S. Kroschwald, C.Y. Chiu, D. Heydeck, N. Rohwer, T. Gehring, U. Seifert, et al., Female mice carrying a defective Alox15 gene are protected from experimental colitis via sustained maintenance of the intestinal epithelial barrier function, *Biochim. Biophys. Acta Mol. Cell Biol. Lipids* 1863 (8) (2018) 866–880.
- [13] L. Zhao, M.P. Moos, R. Grabner, F. Pedrono, J. Fan, B. Kaiser, et al., The 5-lipoxygenase pathway promotes pathogenesis of hyperlipidemia-dependent aortic aneurysm, *Nat. Med.* 10 (9) (2004) 966–973.
- [14] P. Sirois, Leukotrienes: one step in our understanding of asthma, *Respir. Investig.* 57 (2) (2019) 97–110.
- [15] C.N. Serhan, J. Dalli, R.A. Colas, J.W. Winkler, N. Chiang, Protectins and maresins: new pro-resolving families of mediators in acute inflammation and resolution bioactive metabolome, *Biochim. Biophys. Acta* 1851 (4) (2015) 397–413.

- [16] J.A. Ackermann, K. Hofheinz, M.M. Zaiss, G. Kronke, The double-edged role of 12/15-lipoxygenase during inflammation and immunity, *Biochim. Biophys. Acta* 1862 (4) (2017) 371–381.
- [17] J. Cao, E.B. Yang, J.J. Su, Y. Li, P. Chow, The tree shrews: adjuncts and alternatives to primates as models for biomedical research, *J. Med. Primatol.* 32 (3) (2003) 123–130.
- [18] J. Xiao, R. Liu, C.S. Chen, Tree shrew (*Tupaia belangeri*) as a novel laboratory disease animal model, *Zool. Res.* 38 (3) (2017) 127–137.
- [19] Y.G. Yao, Creating animal models, why not use the Chinese tree shrew (*Tupaia belangeri chinensis*)? *Zool. Res.* 38 (3) (2017) 118–126.
- [20] L. Xu, S.Y. Chen, W.H. Nie, X.L. Jiang, Y.G. Yao, Evaluating the phylogenetic position of Chinese tree shrew (*Tupaia belangeri chinensis*) based on complete mitochondrial genome: implication for using tree shrew as an alternative experimental animal to primates in biomedical research, *J Genet Genomics.* 39 (3) (2012) 131–137.
- [21] Y. Fan, Z.Y. Huang, C.C. Cao, C.S. Chen, Y.X. Chen, D.D. Fan, et al., Genome of the Chinese tree shrew, *Nat. Commun.* 4 (2013) 1426.
- [22] Y. Fan, M.S. Ye, J.Y. Zhang, L. Xu, D.D. Yu, T.L. Gu, et al., Chromosomal level assembly and population sequencing of the Chinese tree shrew genome, *Zool Res.* 40 (2019) 506–521.
- [23] F. Zhao, X. Guo, Y. Wang, J. Liu, W.H. Lee, Y. Zhang, Drug target mining and analysis of the Chinese tree shrew for pharmacological testing, *PLoS One* 9 (8) (2014) e104191.
- [24] R. Li, M. Zanin, X. Xia, Z. Yang, The tree shrew as a model for infectious diseases research, *J Thorac Dis.* 10 (Suppl. 19) (2018) (S2272-S9).
- [25] K. Tsukiyama-Kohara, M. Kohara, *Tupaia belangeri* an experimental animal model for viral infection, *Exp. Anim.* 63 (4) (2014) 367–374.
- [26] D.W. Gilroy, D. Bishop-Bailey, Lipid mediators in immune regulation and resolution, *Br. J. Pharmacol.* 176 (8) (2019) 1009–1023.
- [27] H. Kuhn, L. Humeniuk, N. Kozlov, S. Roigas, S. Adel, D. Heydeck, The evolutionary hypothesis of reaction specificity of mammalian ALOX15 orthologs, *Prog. Lipid Res.* 72 (2018) 55–74.
- [28] K. Goloschchapova, S. Stehling, D. Heydeck, M. Blum, H. Kuhn, Functional characterization of a novel arachidonic acid 12S-lipoxygenase in the halotolerant bacterium *Myxococcus fulvus* exhibiting complex social living patterns, *Microbiologyopen.* (2018) e775.
- [29] S. Banthiya, J. Kalms, E. Galemou Yoga, I. Ivanov, X. Carpena, M. Hamberg, et al., Structural and functional basis of phospholipid oxygenase activity of bacterial lipoxygenase from *Pseudomonas aeruginosa*, *Biochim. Biophys. Acta* 1861 (11) (2016) 1681–1692.
- [30] N. Kozlov, L. Humeniuk, C. Ufer, I. Ivanov, A. Golovanov, S. Stehling, et al., Functional characterization of novel ALOX15 orthologs representing key steps in mammalian evolution supports the evolutionary hypothesis of reaction specificity, *Biochim. Biophys. Acta Mol. Cell Biol. Lipids* 1864 (3) (2019) 372–385.
- [31] R. Vogel, C. Jansen, J. Roffeis, P. Reddanna, P. Forsell, H.E. Claesson, et al., Applicability of the triad concept for the positional specificity of mammalian lipoxygenases, *J. Biol. Chem.* 285 (8) (2010) 5369–5376.
- [32] R.W. Bryant, J.M. Bailey, T. Schewe, S.M. Rapoport, Positional specificity of a reticulocyte lipoxygenase. Conversion of arachidonic acid to 15-S-hydroperoxy-eicosatetraenoic acid, *J. Biol. Chem.* 257 (11) (1982) 6050–6055.
- [33] S. Borngraber, M. Browner, S. Gillmor, C. Gerth, M. Anton, R. Fletterick, et al., Shape and specificity in mammalian 15-lipoxygenase active site. The functional interplay of sequence determinants for the reaction specificity, *J. Biol. Chem.* 274 (52) (1999) 37345–37350.
- [34] P. Ludwig, H.G. Holzthutter, A. Colosimo, M.C. Silvestrini, T. Schewe, S.M. Rapoport, A kinetic model for lipoxygenases based on experimental data with the lipoxygenase of reticulocytes, *Eur. J. Biochem.* 168 (2) (1987) 325–337.
- [35] J.D. Deschamps, A.F. Ogunsola, J.B. Jameson 2nd, A. Yasgar, B.A. Flitter, C.J. Freedman, et al., Biochemical and cellular characterization and inhibitor discovery of *Pseudomonas aeruginosa* 15-Lipoxygenase, *Biochemistry.* 55 (23) (2016) 3329–3340.
- [36] I. Juranek, H. Suzuki, S. Yamamoto, Affinities of various mammalian arachidonate lipoxygenases and cyclooxygenases for molecular oxygen as substrate, *Biochim. Biophys. Acta* 1436 (3) (1999) 509–518.
- [37] J. Kalms, S. Banthiya, E. Galemou Yoga, M. Hamberg, H.G. Holzthutter, H. Kuhn, et al., The crystal structure of *Pseudomonas aeruginosa* lipoxygenase Ala420Gly mutant explains the improved oxygen affinity and the altered reaction specificity, *Biochim. Biophys. Acta* 1862 (5) (2017) 463–473.
- [38] M.J. Knapp, J.P. Klinman, Kinetic studies of oxygen reactivity in soybean lipoxygenase-1, *Biochemistry.* 42 (39) (2003) 11466–11475.
- [39] A.L. Tappel, W.O. Lundberg, P.D. Boyer, Effect of temperature and antioxidants upon the lipoxidase-catalyzed oxidation of sodium linoleate, *Arch. Biochem. Biophys.* 42 (2) (1953) 293–304.
- [40] W. Halangk, T. Schewe, C. Hiesch, S. Rapoport, Some properties of the lipoxygenase from rabbit reticulocytes, *Acta Biol Med Ger.* 36 (3–4) (1977) 405–410.
- [41] H. Kuhn, R. Gotze, T. Schewe, S.M. Rapoport, Quasi-lipoxygenase activity of haemoglobin. A model for lipoxygenases, *Eur J Biochem* 120 (1) (1981) 161–168.
- [42] T. Schewe, W. Halangk, C. Hiesch, S.M. Rapoport, A lipoxygenase in rabbit reticulocytes which attacks phospholipids and intact mitochondria, *FEBS Lett.* 60 (1) (1975) 149–152.
- [43] H. Kuhn, J. Belkner, R. Wiesner, A.R. Brash, Oxygenation of biological membranes by the pure reticulocyte lipoxygenase, *J. Biol. Chem.* 265 (30) (1990) 18351–18361.
- [44] J. Belkner, H. Stender, H. Kuhn, The rabbit 15-lipoxygenase preferentially oxygenates LDL cholesterol esters, and this reaction does not require vitamin E, *J. Biol. Chem.* 273 (36) (1998) 23225–23232.

- [45] L. Xu, D. Yu, Y. Fan, L. Peng, Y. Wu, Y.G. Yao, Loss of RIG-I leads to a functional replacement with MDA5 in the Chinese tree shrew, *Proc. Natl. Acad. Sci. U. S. A.* 113 (39) (2016) 10950–10955.
- [46] Y. Han, B. Li, T.T. Yin, C. Xu, R. Ombati, L. Luo, et al., Molecular mechanism of the tree shrew's insensitivity to spiciness, *PLoS Biol.* 16 (7) (2018) e2004921.
- [47] T. Gu, D. Yu, Y. Fan, Y. Wu, Y.L. Yao, L. Xu, et al., Molecular identification and antiviral function of the guanylate-binding protein (GBP) genes in the Chinese tree shrew (*Tupaia belangeri chinensis*), *Dev. Comp. Immunol.* 96 (2019) 27–36.
- [48] C.H. Li, L.Z. Yan, W.Z. Ban, Q. Tu, Y. Wu, L. Wang, et al., Long-term propagation of tree shrew spermatogonial stem cells in culture and successful generation of transgenic offspring, *Cell Res.* 27 (2) (2017) 241–252.
- [49] X. Ma, A.S. Wong, H.Y. Tam, S.Y. Tsui, D.L. Chung, B. Feng, In vivo genome editing thrives with diversified CRISPR technologies, *Zool. Res.* 39 (2) (2018) 58–71.
- [50] S. Adel, F. Karst, A. Gonzalez-Lafont, M. Pekarova, P. Saura, L. Masgrau, et al., Evolutionary alteration of ALOX15 specificity optimizes the biosynthesis of anti-inflammatory and proresolving lipoxins, *Proc. Natl. Acad. Sci. U. S. A.* 113 (30) (2016) E4266–E4275.
- [51] S.M. Rapoport, T. Schewe, R. Wiesner, W. Halangk, P. Ludwig, M. Janicke-Hohne, et al., The lipoxygenase of reticulocytes. Purification, characterization and biological dynamics of the lipoxygenase; its identity with the respiratory inhibitors of the reticulocyte, *Eur. J. Biochem.* 96 (3) (1979) 545–561.
- [52] C. Yokoyama, F. Shinjo, T. Yoshimoto, S. Yamamoto, J.A. Oates, A.R. Brash, Arachidonate 12-lipoxygenase purified from porcine leukocytes by immunoaffinity chromatography and its reactivity with hydroperoxyeicosatetraenoic acids, *J. Biol. Chem.* 261 (35) (1986) 16714–16721.
- [53] M. Pekarova, H. Kuhn, L. Bezakova, C. Ufer, D. Heydeck, Mutagenesis of triad determinants of rat Alox15 alters the specificity of fatty acid and phospholipid oxygenation, *Arch. Biochem. Biophys.* 571 (2015) 50–57.
- [54] M. Johannesson, L. Backman, H.E. Claesson, P.K. Forsell, Cloning, purification and characterization of non-human primate 12/15-lipoxygenases, *Prostaglandins Leukot Essent Fatty Acids.* 82 (2–3) (2010) 121–129.
- [55] T. Watanabe, J.Z. Haeggstrom, Rat 12-lipoxygenase: mutations of amino acids implicated in the positional specificity of 15- and 12-lipoxygenases, *Biochem. Biophys. Res. Commun.* 192 (3) (1993) 1023–1029.
- [56] N.K. Singh, G.N. Rao, Emerging role of 12/15-Lipoxygenase (ALOX15) in human pathologies, *Prog. Lipid Res.* 73 (2019) 28–45.
- [57] I. Ivanov, H. Kuhn, D. Heydeck, Structural and functional biology of arachidonic acid 15-lipoxygenase-1 (ALOX15), *Gene.* 573 (2015) 1–32.
- [58] H. Kühn, J. Barnett, D. Grunberger, P. Baecker, J. Chow, B. Nguyen, et al., Overexpression, purification and characterization of human recombinant 15-lipoxygenase, *Biochim. Biophys. Acta* 1169 (1) (1993) 80–89.
- [59] Y. Takahashi, W.C. Glasgow, H. Suzuki, Y. Taketani, S. Yamamoto, M. Anton, et al., Investigation of the oxygenation of phospholipids by the porcine leukocyte and human platelet arachidonate 12-lipoxygenases, *Eur. J. Biochem.* 218 (1) (1993) 165–171.
- [60] I. Ivanov, D. Heydeck, K. Hofheinz, J. Roffeis, V.B. O'Donnell, H. Kuhn, et al., Molecular enzymology of lipoxygenases, *Arch. Biochem. Biophys.* 503 (2) (2010) 161–174.
- [61] E. Sigal, D. Grunberger, C.S. Craik, G.H. Caughey, J.A. Nadel, Arachidonate 15-lipoxygenase (omega-6 lipoxygenase) from human leukocytes. Purification and structural homology to other mammalian lipoxygenases, *J. Biol. Chem.* 263 (11) (1988) 5328–5332.
- [62] P. Chaitidis, S. Adel, M. Anton, D. Heydeck, H. Kuhn, T. Horn, Lipoxygenase pathways in *Homo neanderthalensis*: functional comparison with *Homo sapiens* isoforms, *J. Lipid Res.* 54 (5) (2013) 1397–1409.
- [63] S. Adel, K.R. Kakularam, T. Horn, P. Reddanna, H. Kuhn, D. Heydeck, Leukotriene signaling in the extinct human subspecies *Homo denisovan* and *Homo neanderthalensis*. Structural and functional comparison with *Homo sapiens*, *Arch. Biochem. Biophys.* 565 (2015) 17–24.
- [64] J. Freire-Moar, A. Alavi-Nassab, M. Ng, M. Mulkins, E. Sigal, Cloning and characterization of a murine macrophage lipoxygenase, *Biochim. Biophys. Acta* 1254 (1) (1995) 112–116.
- [65] N. De Marzo, D.L. Sloane, S. Dicharry, E. Highland, E. Sigal, Cloning and expression of an airway epithelial 12-lipoxygenase, *Am. J. Phys.* 262 (2 Pt 1) (1992) L198–L207.
- [66] H. Suzuki, K. Kishimoto, T. Yoshimoto, S. Yamamoto, F. Kanai, Y. Ebina, et al., Site-directed mutagenesis studies on the iron-binding domain and the determinant for the substrate oxygenation site of porcine leukocyte arachidonate 12-lipoxygenase, *Biochim. Biophys. Acta* 1210 (3) (1994) 308–316.
- [67] D.L. Sloane, R. Leung, C.S. Craik, E. Sigal, A primary determinant for lipoxygenase positional specificity, *Nature.* 354 (6349) (1991) 149–152.
- [68] K. van Leyen, H.Y. Kim, S.R. Lee, G. Jin, K. Arai, E.H. Lo, Baicalein and 12/15-lipoxygenase in the ischemic brain, *Stroke.* 37 (12) (2006) 3014–3018.
- [69] G. Jin, K. Arai, Y. Murata, S. Wang, M.F. Stins, E.H. Lo, et al., Protecting against cerebrovascular injury: contributions of 12/15-lipoxygenase to edema formation after transient focal ischemia, *Stroke.* 39 (9) (2008) 2538–2543.
- [70] K. Yigitkanli, A. Pekcec, H. Karatas, S. Pallast, E. Mandeville, N. Joshi, et al., Inhibition of 12/15-lipoxygenase as therapeutic strategy to treat stroke, *Ann. Neurol.* 73 (1) (2013) 129–135.
- [71] H. Karatas, J. Eun Jung, E.H. Lo, K. van Leyen, Inhibiting 12/15-lipoxygenase to treat acute stroke in permanent and tPA induced thrombolysis models, *Brain Res.* 1678 (2018) 123–128.
- [72] Gaberel T, Gakuba C, Zheng Y, Lepine M, Lo EH, van Leyen K. Impact of 12/15-Lipoxygenase on brain injury after subarachnoid hemorrhage. *Stroke.* 2019;50(2):520–3.
- [73] Y. Liu, Y. Zheng, H. Karatas, X. Wang, C. Foerch, E.H. Lo, et al., 12/15-Lipoxygenase inhibition or knockout reduces warfarin-associated hemorrhagic transformation after experimental stroke, *Stroke.* 48 (2) (2017) 445–451.
- [74] R.L. Haynes, K. van Leyen, 12/15-lipoxygenase expression is increased in oligodendrocytes and microglia of periventricular leukomalacia, *Dev. Neurosci.* 35 (2–3) (2013) 140–154.
- [75] K. van Leyen, K. Arai, G. Jin, V. Kenyon, B. Gerstner, P.A. Rosenberg, et al., Novel lipoxygenase inhibitors as neuroprotective reagents, *J. Neurosci. Res.* 86 (4) (2008) 904–909.
- [76] G. Rai, N. Joshi, J.E. Jung, Y. Liu, L. Schultz, A. Yasgar, et al., Potent and selective inhibitors of human reticulocyte 12/15-lipoxygenase as anti-stroke therapies, *J. Med. Chem.* 57 (10) (2014) 4035–4048.
- [77] Y.B. Joshi, P.F. Giannopoulos, D. Pratico, The 12/15-lipoxygenase as an emerging therapeutic target for Alzheimer's disease, *Trends Pharmacol. Sci.* 36 (3) (2015) 181–186.
- [78] A. Di Meco, J.G. Li, B.E. Blass, M. Abou-Gharbia, E. Lauretti, D. Pratico, 12/15-Lipoxygenase inhibition reverses cognitive impairment, brain amyloidosis, and tau pathology by stimulating autophagy in aged triple transgenic mice, *Biol. Psychiatry* 81 (2) (2017) 92–100.
- [79] Y. Fan, R. Luo, L.Y. Su, Q. Xiang, D. Yu, L. Xu, et al., Does the genetic feature of the Chinese tree shrew (*Tupaia belangeri chinensis*) support its potential as a viable model for Alzheimer's disease research? *J. Alzheimers Dis.* 61 (3) (2018) 1015–1028.
- [80] E. Birney, M. Clamp, Durbin R. GeneWise, Genomewise, *Genome Res.* 14 (5) (2004) 988–995.
- [81] Y. Fan, D. Yu, Y.G. Yao, Tree shrew database (TreeshrewDB): a genomic knowledge base for the Chinese tree shrew, *Sci. Rep.* 4 (2014) 7145.
- [82] E.G. Bligh, W.J. Dyer, A rapid method of total lipid extraction and purification, *Can. J. Biochem. Physiol.* 37 (8) (1959) 911–917.
- [83] Y.L. Yao, D. Yu, L. Xu, Y. Fan, Y. Wu, T. Gu, et al., Molecular characterization of the 2',5'-oligoadenylate synthetase family in the Chinese tree shrew (*Tupaia belangeri chinensis*), *Cytokine.* 114 (2019) 106–114.

# Supplementary Data

**Figure S1A: Multiple amino acid alignments of tupALOX-isoforms with human and mouse ALOX15 orthologs.** The direct iron liganding amino acids are indicated in blue. The triad determinants of the reaction specificity are labeled in yellow. The *tupD1-Alox15* gene encodes for the enzyme, which is named tupALOX15a in this study. Similarly, the *tupD2-Alox15* encodes for the enzyme named tupALOX15b in this study. The *tupD3-Alox15* gene encodes for the enzyme tupALOX15c and the *tupD4-Alox* gene encodes for tupALOX15d.

MouseAlox15	MGVYRIRVSTGDSVYAGSNNEVYLWLIGQHGEASLGKLFRCRNSEAEFKVDVSEYLGPL	60
HumALOX15	MGLYRIRVSTGASLYAGSNNQVQLWLVGQHGEAALGKRLWPARGKETELKVEVPEYLGPL	60
TupD2_Alox15	MVLYRIRVSTGSSCYAGSKNQVHLSLVGQHGEAALGWRLRPGAGQ-GEFQVDVQYELGPL	59
TupD4_Alox15	MVLYRIRVSTGSSCYAGSKNQVHLSLVGQHGEAALGWRLRPARGKVEEFQVDVQYELGPL	60
TupD1_ALOX15	MVLYRIRVSTGSSCYAGSKNQVHLSLVGQHGEAALGWRLRPARGKVEEFQVDVQYELGPL	60
TupD3_Alox15	MVLYRIRVSTGSSCYAGSKNQVHLSLVGQHGEAALGWRLRPARGKVEEFQVDVQYELGPL	60
	* :***** * ****:* * * :*****:** : * .: * :* * *****	
MouseAlox15	LFVVRQKWHYLKEDAWFCNWI SVKGPQGDSSEYTFPCYRWVQGTSLNLNPEGTGCTVVED	120
HumALOX15	LFVKLRKRHLLKDDAWFCNWI SVQGPQA-GDEVRFPCYRWVEGNGVLSLPEGTGRTVGED	119
TupD2_Alox15	LFVKLRKRHLLQDDAWFCNWI SVQGPQASGDEVRFPCYRWVEGKDI LSLPEATGRTVVD	119
TupD4_Alox15	LFVKLRKRHLLQDDAWFCNWI SVQGPQARGDEVRFPCYRWVEGKDI LNLPEATGRTVVD	120
TupD1_ALOX15	LFVKLRKRHLLQDDAWFCNWI SVQGPQASGDEVRFPCYRWVEGKDI LSLPEATGRTVVD	120
TupD3_Alox15	LFVKLRKRHLLQDDAWFCNWI SVQGPQASGDEVRFPCYRWVEGKDI LSLPEATGRTVVD	120
	***: : * * * :*****:**:** * * * * * :* .: * .** * * * * :*	
MouseAlox15	SQGLFRNHREEELEERRSLYRWGNWKDGT IILNVAATSISDLPVDQRFREDKRLEFEASQV	180
HumALOX15	PQGLFQKHREEELEERRKLYRWGNWKDGLI LNMAGAKLYDLPVDERFLEDKRVDFEVSLA	179
TupD2_Alox15	PQGLFRRHREEELEDRKKVYRWGNWKDGLI LNMAGPGLNDLPVDERFLEDKRIDFEASLA	179
TupD4_Alox15	PQGLFRRHREEELEDRKKVYRWGNWKDGLI LNVAGACINDLPVDERFLEDKRIDFEASLA	180
TupD1_ALOX15	PQGLFRRHREEELEDRKKVYRWGNWKDGLI LNMAGPGLNDLPVDERFLEDKRIDFEASLA	180
TupD3_Alox15	PEGLFRRHREEELEDRKKVYRWGNWKDGLI LNMAGAGLNDLPVDERFLEDKRIDFEASLA	180
	:***: .*****:* :***** **:* . : *****:* *****:*** * .	
MouseAlox15	LGTMDTVINFPKNTVTCWKSLLDDFNVFKSGHTKMAERVRNSWKEDAFFGYQFLNGANPM	240
HumALOX15	KGLADLAIKDSLNLVTCWKLLDDFNRI FWCGQSKLAERVRDSWKEDALFGYQFLNGANPV	239
TupD2_Alox15	KGLAELAIAKDSLNI LANWNNVDDFNRI FWCGPSKLAQVVRDSWKEDALFGYQFLNGANPM	239
TupD4_Alox15	KGLAELAIAKDSLNI LANWNNVDDFNRI FWCGPSKLAQVVRDSWKEDALFGYQFLNGANPM	240
TupD1_ALOX15	KGLAELAIAKDSLNI LANWNNVDDFNRI FWCGPSKLAQVVRDSWKEDALFGYQFLNGANPM	240
TupD3_Alox15	KGLAELAIAKDSLNI LANWNNVDDFNRI FWCGPSKLAQVVRDSWKEDALFGYQFLNGANPM	240
	* : .*: * : : * :*****: * * * * * :* :* :* :* :*****:*****:**:	
MouseAlox15	VLKRSTCLPARLVFPPGMEKIQALDEELKKGTLFEADFFLLDGIKANVILCSQQYLAAAP	300
HumALOX15	VLRSSAHLPARLVFPPGMEELQAQLEKELEGGTLFEADFFLLDGIKANVILCSQQHLAAAP	299
TupD2_Alox15	LLRRSCHLPDRLVFPFPGMEELRAQLENELRAGTLFEADYSLLDGIKANVILCRQQYLAAAP	299
TupD4_Alox15	LLRRSCHLPDRLVFPFPGMEELRAQLENELRAGTLFEADYSLLDGIKANVILCRQQYLAAAP	300
TupD1_ALOX15	LLRRSCHLPDRLVFPFPGMEELRAQLENELRAGTLFEADYSLLDGIKANVILCRQQYLAAAP	300
TupD3_Alox15	LLRRSQLPDRLVFPFPGMEELRAQLENELRAGTLFEADYSLLDGIKANVILCRQQYLAAAP	300
	:** * * *****:* :***:**. *****: ***** ***** **:***	
MouseAlox15	LVMLKLPDQGLLPIAIQLELPKGTSTPPPIFTPLDPPMDWLLAKCWVRSDFQLHELQA	360
HumALOX15	LVMLKLPDQGLLPMVIQLQLPRTGSPPPPLFLPTDPPMALLAKCWVRSDFQLHELQS	359
TupD2_Alox15	LVMLKLPDQGLLPMVIQLQLPQGGSPPTLFLPTDPELTWLLAKCWVRSDFQIHELQY	359
TupD4_Alox15	LVMLKLPDQGLLPMVIQLQLPKRGSLLPTLFLPTDPELTWLLAKCWVRSDFQVHELQY	360
TupD1_ALOX15	LVMLKLPDQGLLPMVIQLQLPQGGSPPTLFLPTDPELTWLLAKCWVRSDFQIHELQY	360
TupD3_Alox15	LVMLKLPDQGLLPMVIQLQLPQGGSPPTLFLPTDPELTWLLAKCWVRSDFQVHELQY	360
	***** **:***:.***:** * * * * * : *****:*****:***:**	
MouseAlox15	HLLRGHLVAEVFAVATMRCCLPSVHPVFKLLVPHLLYTMEINVRARSDLISERGFDFKVVMS	420
HumALOX15	HLLRGHLMAEVIIVVATMRCCLPSIHPIFKLIIPHLRYTLEINVRARTGLVSDMGIFDQVMS	419
TupD2_Alox15	HLLRGHLMAEVIIVATMRCCLPSVHPVFKLIVPHLRYTMEINVRARNGLVSDYGVFDQVVS	419
TupD4_Alox15	HLLRGHLMAEVIIVATMRCCLPSVHPVFKLIVPHLRYTMEINVRARNGLVSDYGVFDQVVS	420
TupD1_ALOX15	HLLRGHLMAEVIIVATMRCCLPSVHPVFKLIVPHLRYTMEINVRARNGLVSDYGVFDQVVS	420
TupD3_Alox15	HLLRGHLMAEVIIVATMRCCLPSVHPVFKLIVPHLRYTMEINVRARNGLVSDYGVFDQVVS	420
	*****:**:*****:**:**:** * * * * * : *****: .*: * :* :* :*	

MouseAlox15	TGGGGHLLDLLKQAGAFITYSSLCPPDDLAERGLLDIDTCFYAKDALQLWQVMN-RYVVMG	479
HumALOX15	TGGGGHVQLLKQAGAFITYSSFCPPDDLADRGLLGKSSFYAQDALRLWEI IY-RYVEGI	478
TupD2_Alox15	TGGGGHVEFLKRAKDVLTYSRLCPPDDLADRGLLGQSSYYGQDALRLWEI ILYGRYVEGI	479
TupD4_Alox15	TGGGGHVEFLKRAKGVLTYSRLCPPDDLADRGLLGQSSYYGQDALRLWEI ILYG-YVEGI	479
TupD1_ALOX15	TGGGGHVEFLKRAKDVLTYSRLCPPDDLADRGLLGQSSYYGQDALRLWEI ILYG-YVEGI	479
TupD3_Alox15	TGGGGHVEFLKRAKDVLTYSRLCPPDDLADRGLLGQSSYYGQDALRLWEI ILYG-YVEGI *****::**:* .*** *:*****:****.:...:*.:**:***:***:: ** *:	479
MouseAlox15	FDLYYKTDQAVQDDYELQSWCQEITEIGLQGAQDRGFPTSLQSRQAACHFITMCI FTCTA	539
HumALOX15	VSLHYKTDVAVKDDPELQTWCREITEIGLQGAQDRGFVPSLQARDQVCHFVITMCI FTCTG	538
TupD2_Alox15	VKIHYKSDETVKSDLELQSWCREITEIGLLGAEDRGFPQSLQSLDQLCKFATMCI FTCTG	539
TupD4_Alox15	VKIHYKSDETVKSDLELQSWCREITEVGLLGAEDRGFPKSLQSLDQLCKFATMCI FTCTG	539
TupD1_ALOX15	VKIHYKSDETVKSDLELQSWCREITEIGLLGAEDRGFPKSLQSLDQLCKFATMCI FTCTG	539
TupD3_Alox15	VKIHYKSDETVKSDLELQSWCREITEIGLLGAEDRGFPKSLQSLDQLCKFATMCI FTCTG ...:**:* :*:* ***:**:****:* **:****** ***: * *:* *****.	539
MouseAlox15	QHSSIH LGQLDWFYVWPNA PCTMR LPPPKTKDATMEKLMATLPNPNQSTLQIN VVWLLGR	599
HumALOX15	QHSAVHLGQLDWYSWVWPNA PCTMR LPPPTTKDATLETVMATLPNFHQASLQMS ITWQLGR	598
TupD2_Alox15	QHSSITHMGLDWYAWVWPNA PCTMR MPPPTTKDVTMETVMASLPSVHQASVQMS ITWQLGR	599
TupD4_Alox15	QHSSNHLGQLDWYAWVWPNA PCTMR I PPPTTKDVTMETVMASLPSVHQASVQMS ITWQLGR	599
TupD1_ALOX15	QHSSNHLGQLDWYAWVWPNA PCTMR I PPPTTKDVTMETVMASLPSVHQASLQMS ITWQLGR	599
TupD3_Alox15	QHSSNHLGQLDWYAWVWPNA PCTMR I PPPTTKDVTMETVMASLPSVHQASLQMS ITWQLGR **:* *:******: *****:***.***.*:*:*:**:***. :*:*:*:*:* **	599
MouseAlox15	RQAVMVLPGQHSEEHFPNPEAKAVLKKFREELAALDKEIEIRNKSLDIPYEYLRPSLVEN	659
HumALOX15	RQPVMVAVGQHEEEYFSGPEPKAVLKKFREELAALDKEIEIRNAKLMPYEYLRPSVVEN	658
TupD2_Alox15	RQPFMVALGQHEEEYFSDPASKAVLKT FREKLAAMDKID DARNATLTMPYEYLRPSLVEN	659
TupD4_Alox15	RQPI MVALGQHEEEYFSDPASKAVLKT FREKLAAMDKDV DARNAKLAMPYEYLRPSLVEN	659
TupD1_ALOX15	RQPI MVALGQHEEEYFSDPASKAVLKT FREKLAAMDKDV DARNATLAMPYEYLRPSLVEN	659
TupD3_Alox15	RQPI MVALGQHEEEYFSDPASKAVLKT FREKLAAMDKDV DARNATLAMPYEYLRPSLVEN ** .** :***.***:* .* *****.***:***:**:*** ** .* :*****:**:***	659
MouseAlox15	SVAI	663
HumALOX15	SVAI	662
TupD2_Alox15	SVTI	663
TupD4_Alox15	SVAI	663
TupD1_ALOX15	SVAI	663
TupD3_Alox15	SVAI	663
	**:*	

**Figure S1B: Evolutionary relatedness of tupaia ALOX15 isoforms and their relation to mouse and human ALOX15.**

